PALAIOS
Emphasizing the impact of life on Earth's history

PALAIOS, 2017, v. 32, 413–428
Research Article
DOI: http://dx.doi.org/10.2110/palo.2016.089

OSTRACODE BIOFACIES AND SHELL CHEMISTRY REVEAL QUATERNARY AQUATIC TRANSITIONS IN THE POZUELOS BASIN (ARGENTINA)

MICHAEL M. McGLUE,[1] MANUEL R. PALACIOS-FEST,[2] GABRIELA C. CUSMINSKY,[3] MARIA CAMACHO,[4] SARAH J. IVORY,[1,5] ANDREW L. KOWLER,[6] AND SUVANKAR CHAKRABORTY[7]

[1]*University of Kentucky, Department of Earth and Environmental Sciences, Lexington, Kentucky 40506, USA*
[2]*Terra Nostra Earth Sciences Research LLC, Tucson, Arizona 85740, USA*
[3]*INIBIOMA-CONICET and Centro Regional Universitario de Bariloche, Universidad Nacional de Comahue, Quintral, San Carlos de Bariloche, Argentina*
[4]*Universidad Nacional de Jujuy, Facultad de Ingeniería, San Salvador de Jujuy, Jujuy, Argentina*
[5]*Brown University, Department of Earth, Environmental, and Planetary Sciences, Providence, Rhode Island 02912, USA*
[6]*University of California-Los Angeles, Department of Earth, Planetary, and Space Sciences, Los Angeles, California 90095, USA*
[7]*University of Utah, Department of Geology and Geophysics, Salt Lake City, Utah 84112, USA*
email: michael.mcglue@uky.edu

ABSTRACT: **Here we present the first use of calcareous microfossils to examine the late Quaternary paleoecology of the endorheic Pozuelos Basin (Argentina). Modern deposition in the basin centers on Laguna de los Pozuelos (LP), a shallow playa-lake that is fed by axial rivers and groundwater and dominantly accumulates siliciclastic sediments. Today, the distribution of limnocytherid and cypridoidean ostracodes across southern LP is strongly influenced by distance to the Río Cincel delta, whereas the northern end of the playa-lake is characterized by a paucity of ostracodes due to frequent sub-aerial exposure. Ten ostracode biofacies define a sediment core retrieved from LP, which reveal progressive changes in aquatic environments that varied in salinity, depth, and proximity to deltas over the late Pleistocene. Closed lakes occupied the basin from ~ 37.6–30.7 ka, ~ 28.0–25.0 ka, and ~ 23.0–16.6 ka, whereas saline wetlands occurred when these lakes contracted. Extant LP has no analog in the late Pleistocene record; it formed after ~ 7.2 ka, following a hiatus that removed the Pleistocene–Holocene transition. Paleoecological evidence indicates that the core site was influenced by deltaic inflows from the eastern basin margin until ~ 24.3 ka, an area where today dry alluvial fans are found. Reorganization of the watershed by normal faulting, most likely at ~ 18.0 ka, appears to have reduced the influence of these deltaic inflows. Extensional neotectonics, perhaps induced by incorporation of the Pozuelos Basin into the Andean hinterland, is a mechanism that along with tropical climate change is potentially important to water balance and ecology in high-altitude convergent orogenic basins.**

INTRODUCTION

The high-altitude Puna Plateau (northern Argentina) contains several different classes of sedimentary basin whose strata archive the environmental history of central Andes since the Paleogene. These basins commonly contain several km of continental deposits, usually produced by axial rivers that run parallel to the dominant structural trend, or by centralized lakes and wetlands of variable hydrochemistry (Rigsby et al. 2005; Quade et al. 2008; Cohen et al. 2014). Whereas retroarc foreland basins and their syn-orogenic sediments provide direct evidence for the presence and age of a fold-and-thrust belt (e.g., DeCelles and Giles 1996; DeCelles and Horton 2003), the strata of hinterland basins (*sensu* Horton 2012) provide sedimentary, structural, and volcanic evidence for deep-seated geodynamic processes affecting the growth and uplift of the orogen, such as slab foundering (DeCelles et al. 2014; Schoenboem and Carrapa 2014). Similarly, bedded evaporites deposited in ancient intramontane salt lakes have been put forward as evidence for the early Cenozoic uplift and aridification of the Puna (Alonso et al. 1991; Vandervoort et al. 1995). However, the context of hinterland basins within Cordilleran orogenic systems and their cycles of evolution have only very recently been recognized (DeCelles et al. 2009). As a result, very few studies have considered how late Quaternary strata do, or do not, reflect signals of tectonic change on hydrology in hinterland basins. Clarifying the influence of hinterland tectonic processes on sedimentation patterns are critical for understanding the true influence of tropical climate change on the high Andean plateau (Baker and Fritz 2015).

In this study, we examined late Quaternary deposits from the semi-arid Pozuelos Basin, a hinterland transitional basin on the eastern margin of the Puna in northwestern Argentina (Igarzabal 1978; Fig. 1). In the Andes, numerous hinterland basins have formed between the magmatic arc to the west and the craton-directed thrust belt to the east (Horton 2012). Cohen et al. (2014) noted that although the Pozuelos Basin is bounded by linear thrust faults typical of piggyback basins (*sensu* Ori and Friend 1984), its altitude and patterns of recent deformation allow for a more nuanced

Published Online: June 2017
 0883-1351/17/032-413/$03.00

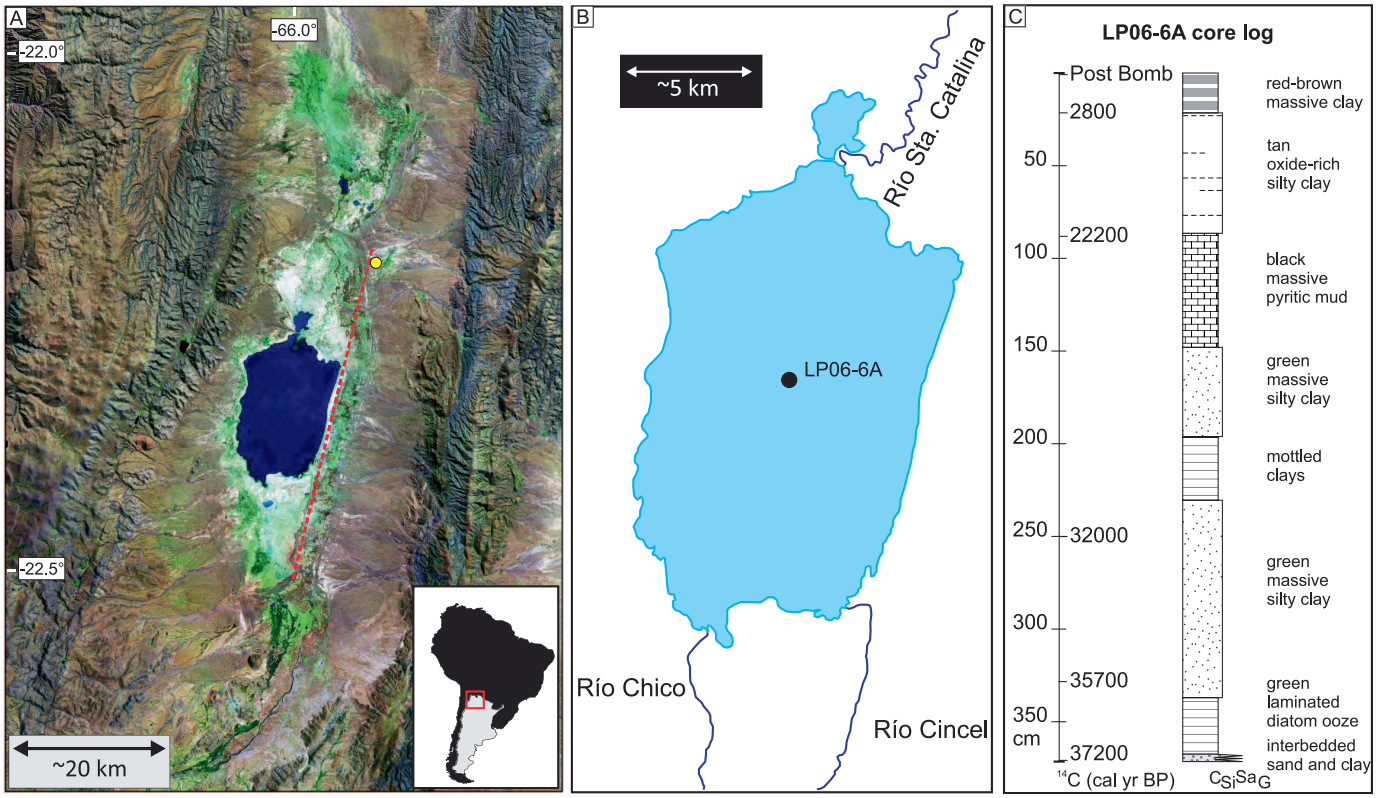

FIG. 1.—**A**) Landsat TM image of the study area. A box defines the location of Laguna de los Pozuelos. A yellow dot marks the location of the Arroyo Corral Blanco, a potential candidate channel for one paleo-river that entered Pleistocene lake phases from the east. Normal fault trace is marked by a dashed line. **B**) Map of extant Laguna de los Pozuelos and its axial drainages. **C**) Stratigraphic log of core LP06-6A, with horizons dated by radiocarbon.

"hybrid" classification of basin type. Several Puna and Altiplano basins fall into this transitional classification, including the Pozuelos and Titicaca Basins (Fig. 1). Modern depositional environments in these basins provide a snapshot of end-member lacustrine sedimentation. Lake Titicaca has been studied through extensive seismic surveying and scientific drilling (Baker et al. 2001a), and the relatively deep and fresh extant lake is a keystone sedimentary and micropaleontological archive (particularly for diatoms and pollen) for the tropical Andes (Paduano et al. 2003; Fritz et al. 2007). Broad subsidence and localized normal faulting are thought to play minor roles in control of stratigraphy relative to changes in insolation and Atlantic sea surface temperatures, which strongly influence the intensity of monsoon precipitation and lake levels (Seltzer et al. 1998; D'Agostino et al. 2002). The Pozuelos Basin, by contrast, is a much more shallow and saline system on the spectrum of lacustrine hinterland transitional basins. Studies of this basin have been far less comprehensive. The absence of a deep modern lake has prevented high resolution seismic profiling, although deep-penetrating, low-resolution seismic lines have imaged much of the syn-orogenic stratigraphic package and high angle structures that may be extensional faults (Gangui 1998); other normal faults have also been identified on the basin flanks (Caffe et al. 2002). A facies analysis on Laguna de los Pozuelos (LP), situated in the center of the Pozuelos Basin, by McGlue et al. (2013) suggested that Quaternary deformation of the basin may have influenced depositional patterns and paleogeography, in addition to climatic influences from dynamics of the summer monsoon. However, a thorough analysis of ancient biota from the Pozuelos Basin has never been attempted, fundamentally limiting our understanding of environmental change and its influence on this high-altitude aquatic ecosystem. Understanding the sensitivity of the ancient Pozuelos ecosystem may also benefit conservation management today, as this area is recognized by the Ramsar Convention as a wetland of international importance. Therefore, we focused our research on late Quaternary calcareous microfossil (ostracodes and charophytes) bearing strata from the subsurface of Laguna de los Pozuelos (Fig. 1).

Ostracodes are microscopic crustaceans characterized by a hinged calcitic carapace that varies in size (~ 0.5–2 mm) and is frequently well-preserved in the rock record (Pokorný 1978; Horne et al. 2002). Ostracodes colonized continental aquatic systems as early as the Carboniferous, and today the group is diverse and abundant within both marine and nonmarine environments alike. Continental ostracodes are mostly benthic, although a few species are nektic and may swim around vegetation (Forester 1991). Physiological responses to water temperature, pH, salinity, dissolved CO_2, dissolved O_2, nutrients, and trophic levels usually control ostracode diversity and abundance, making them very useful as paleoenvironmental indicators (De Deckker and Forrester 1988; Palacios-Fest et al. 1994; Holmes and Chivas 2002; Schwalb 2003). The Online Supplemental File provides ecological characteristics of the ostracode species found in Laguna de los Pozuelos.

De Deckker (2002) warns about the taphonomic effects responsible for shell damage during burial processes, which can influence paleoecological interpretations. For example, when the organism dies, sediments covering the remains may apply sufficient pressure to cause shell damage. Bacterial activity may also weaken the structure post mortem, by producing trails as chitinous tissues around the mineral composition of the shell is consumed. Corrosion is another major factor in shell dissolution. This may occur under acidic, alkaline, or eutrophic conditions. Redox factors may also damage the potential fossils by encrusting exotic minerals like pyrite, gypsum, or calcite (Oertli 1971; Puri 1974; Horne et al. 2002). Whatley (1983) and Brouwers (1988) offer some ideas on identifying these

taphonomic factors in the geologic record. Recognizing abrasion, fragmentation, and corrosion is possible through microscope analysis. These may be identified through streaks or trails on the shell surface, degree of fragmentation (which can be confounded by sample washing and specimen preparation), and mineral encrustation. Population structure (adult-to-juvenile ratios), disarticulation (carapace-to-valve ratios), and species diversity may also help recognize taphonomic effects (e.g., species endowed with robust shells may resist degradation; De Deckker 2002).

Similarly, the calcareous remains of Characeae, macroscopic green algae, have also been exploited for reconstructions of lake water alkalinity, Mg/Ca, and nutrient budgets. Charophytes can contribute significantly to the biomass of shallow lakes; the average height of these macrophytes live is 30–45 cm, and dense meadows are known from a variety of modern environments (Krause 1997; van der Berg et al. 1999; Rip et al. 2007). Ecologically, the Charophyta promote water clarity, enhance fish populations, stabilize lake floors, and most important to the geological record, make significant contributions to biochemical sedimentation (e.g., von Grafenstein et al. 2000). Species of the genus *Chara* tend to be the most morphologically complex of the charophytes, and produce heavy calcareous encrustations along the axis of the thalli, as well as on the gyrogonites, associated with the female reproductive organs (oogonia). These encrustations have given rise to the name stoneworts (Cohen 2003). Usually, charophytes grow in shallow waters (< 60 cm deep) and have short growing seasons limited by water availability and warm temperatures. The fossil record of charophytes extends to the late Silurian, but they have been heavily exploited for Tertiary and Quaternary lake studies (Anadón et al. 2000; Apolinarska and Hammarlund 2009).

The goal of this paper is to clarify how patterns of ecology and hydrology in the Pozuelos Basin (PB) were impacted by tectonic and climatic change in the late Quaternary. Our primary tool for this analysis was the development of a new biofacies and geochemical record from a basin-center sediment core from LP. We used ostracodes, *Chara*, and carbon and oxygen stable isotope ratios from *Limnocythere lysandrosi*, a new, potentially endemic ostracode species present throughout the stratigraphic column, to resolve poorly addressed questions on the timing and causes of paleohydrological changes. The recently produced taxonomic key of Palacios-Fest et al. (2016) guided this analysis (Fig. 2). Geochronological control leveraged an existing radiocarbon database that is improved upon by Bayesian modeling of age-depth relationships. We also supplement the sediment core data with insights from Quaternary outcrops along the eastern margin of the basin to provide a more comprehensive spatial perspective of the controls on depositional patterns over the past ~ 40.0 ka. The results demonstrate that hinterland tectonic deformation can alter surface water networks and spur important changes in lacustrine ecology in the Puna and analogous sites in other cordilleran orogenic belts.

SETTING

The endorheic Pozuelos Basin is located on the high-altitude (> 3500 m asl) Puna Plateau. The basin formed by thrust faulting and associated subsidence during the Oligocene, but evidence of younger extensional faults and volcanism are present in the basin (Cladouhos et al. 1994; Gangui 1998). Neogene ignimbrites occur along the eastern margin of the basin, whereas the western basin margin is dominated by Ordovician siliciclastic and volcanic rocks. Miocene continental deposits are exposed along the eastern basin margin and form a potential source of hard water to LP. Climate patterns in the region are characterized by aridity and relatively cold temperatures (monthly mean temperatures from 3 to 13°C; Legates and Willmott 1990a, 1990b). The arrival of rainfall depends primarily on the South American summer monsoon (Zhou and Lau 1998). The basin typically receives ~320 mm of rainfall each year, with about 70% occurring during the austral summer. The El Niño Southern Oscillation and North Atlantic sea surface temperatures help to regulate patterns of modern precipitation over the Pozuelos Basin (Garreaud et al. 2009).

METHODS

The floor of the Pozuelos Basin was extensively sampled and percussion-cored during the austral winter months of 2006 and 2007 (McGlue et al. 2012; McGlue et al. 2013). For the present study, we investigated ostracodes and calcareous algae in modern sediment samples (n = 9) collected by scoop sampler at stations reflecting different geomorphological sub-environments of southern LP, including the playa-lake center, marginal mudflats, and deltaic settings (Fig. 3). Standing water is much more common in the southern half of LP, due to the relatively steady baseflow from the Río Cincel. Core top sediments (n = 5) from the northern end of the playa-lake were also analyzed, as this region is frequently sub-aerially exposed. Insights from the modern samples were used to calibrate interpretations of biofacies and carapace stable isotope chemistry made on late Quaternary sediment core samples.

Thirty-four samples from core LP06-6A were selected for micropaleontological analysis. This core was retrieved from the central axis of LP (22°S, 66°W). The vertical spacing between each sub-sample varied from 10–15 cm. The initial radiocarbon (^{14}C) chronology of LP06-6A, based on linear interpolation between ^{14}C means, was presented in McGlue et al. (2013). Here, we improve the age model using the Bayesian age-depth modeling software BACON in R (Blaauw and Christen 2011). The ^{14}C dates were calibrated using SHCal13, due to the location of the site in the southern hemisphere (Hogg et al. 2013), and the single post-bomb date at the top of the core was calibrated using the SH3 post-bomb calibration curve (Hua et al. 2013). The BACON program estimates sediment accumulation rates through millions of Monte Carlo Markov Chain (MCMC) iterations. The advantage of Bayesian modeling for age-depth pair construction is that prior information concerning hiatuses and accumulation rates, modeled as gamma distributions, can be accounted for in the analysis. Indications in the stratigraphy as well as geochemical data suggest a hiatus at the transition to deposition of recent playa-lake muds (McGlue et al. 2013). Interpolation between ^{14}C dates above and below this depth show different slopes, suggesting slower accumulation rates when deposition recommenced after the hiatus. Due to these observations, we set a depth for a hiatus at 28 cm and ran the BACON model using default prior information for all parameters except the mean accumulation rates (Goring et al. 2012). Based on previous work in the basin, the accumulation rate priors were modeled as gamma distributions with means of 200 yrs/mm above and 100 yrs/mm below the hiatus. The model output showed a stationary distribution in the MCMC iterations, suggesting that this parametrization fits the data well. The weighted mean age-depth model, with 95% confidence intervals, is plotted in Figure 4.

The samples for micropaleontological analyses were prepared using routine procedures (Forester 1988; Palacios-Fest 1994). The sediments were air-dried, weighed, and disaggregated in boiling water with 1 g of Alconox®. The samples were then allowed to sit in the Alconox solution at room temperature for five days; each sample was gently stirred once per day. Following disaggregation, the samples were separated by size by washing them through a set of coarse (> 1 mm), medium (> 106 μm), and fine (> 63 μm) sieves. The residual material was analyzed under a low-power microscope in order to identify the fossil content. Whenever possible, ostracodes and the gyrogonites of calcareous algae were identified to the species level. At least 300 counts were made per sample, although in rare cases this was not possible. All species were described using standard taxonomic keys for each group, measured, and photographed for illustration. The taxonomy of ostracodes encountered in LP is discussed in Palacios-Fest et al. (2016).

Four statistical indices of diversity and similarity were used to compare faunal assemblages. Population density is the estimated number of valves

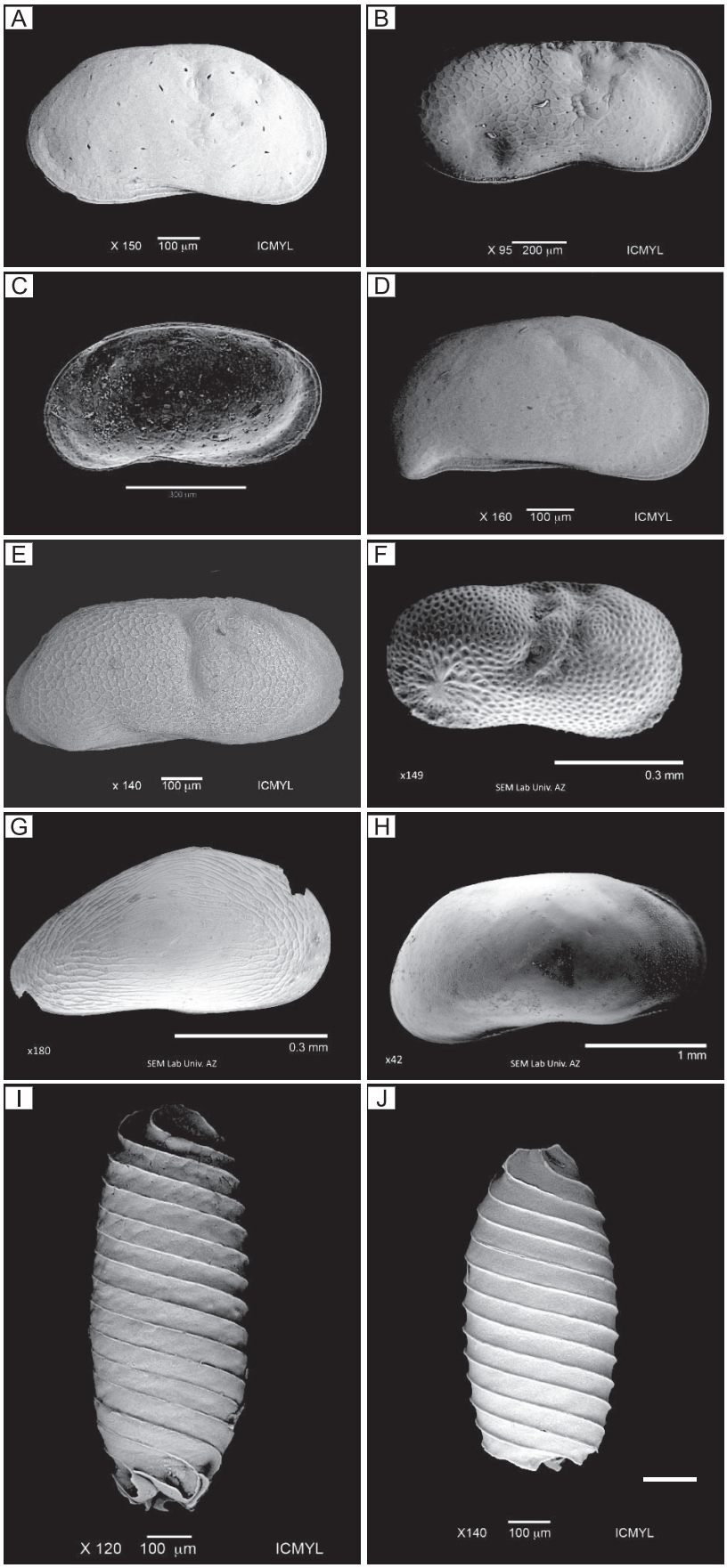

FIG. 2.—Calcareous microfossils recovered in core LP06-6A. **A**) Adult female *Limnocythere alexanderi*. **B)** Adult male *Limnocythere lysandrosi*. **C**) Adult male *Limnocythere foresteri*. **D**) Adult male *Limnocythere ruipunctifinalis*. **E**) Adult female *Limnocythere titcaca*. **F**) Adult female *Ilyocypris ramirezi*. **G**) Adult *Eucypris virgata*. **H**) Pre-adult *Chlamydotheca pseudobrasiliensis*. **I**) *Chara filiformis*. **J**) *Chara vulgaris*. See Palacios-Fest et al. (2016) for details.

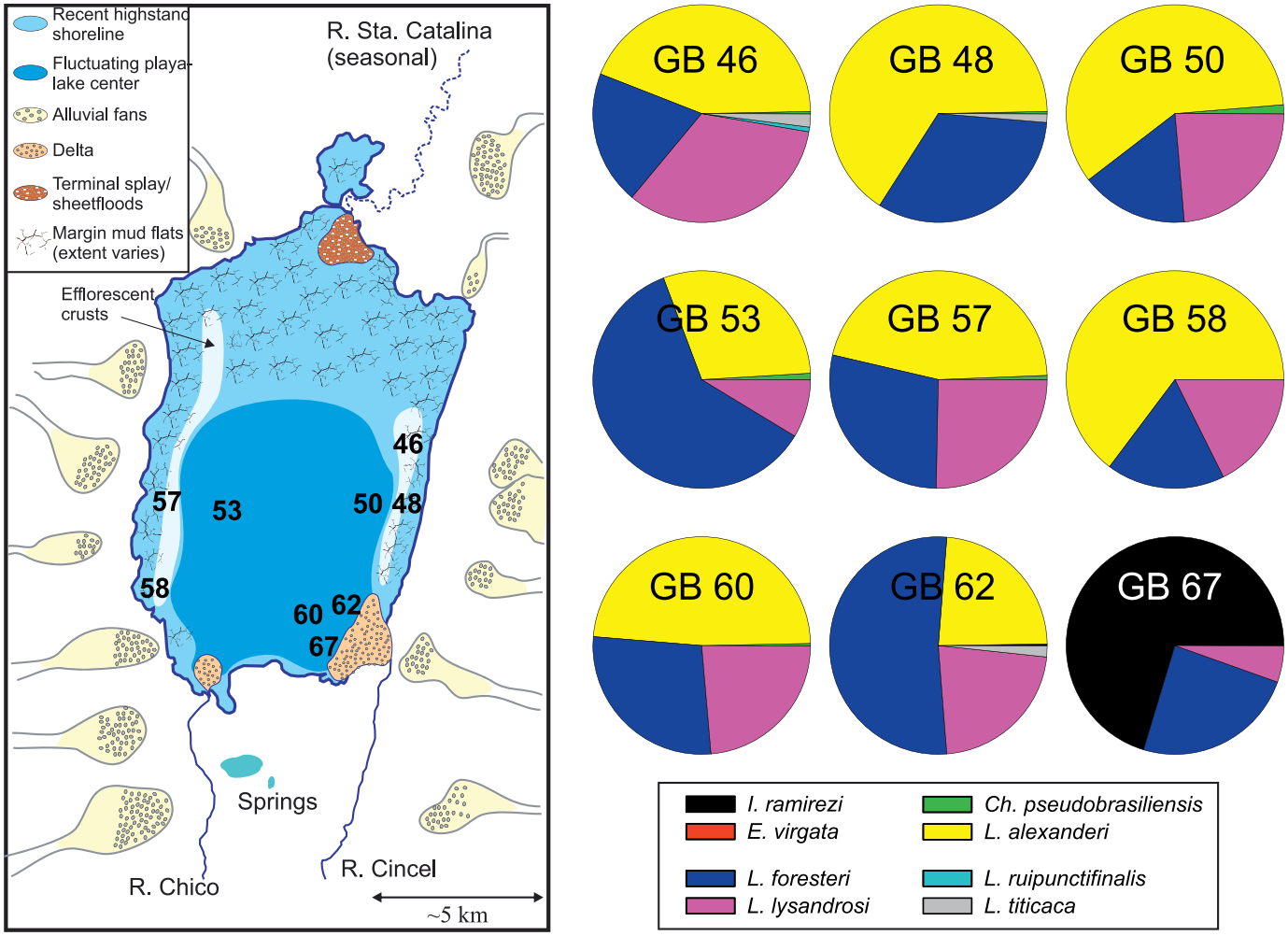

FIG. 3.—Modern ostracode assemblages of Laguna de los Pozuelos. Facies map (left) shows the location of sampling stations on the basin floor (modified after McGlue et al. 2012). Pie charts (right) relate the number and abundance of species encountered at individual stations. Cypridoidean ostracodes are most abundant adjacent to the Río Cincel delta.

per gram of sample (organisms/g), whereas the raw samples species richness is the number of species encountered per sample, uncorrected for sample size. Fisher's α Diversity Index compensates for variations in sample size for the purpose of comparing diversity among variable samples, and is expressed by:

$$\alpha = N(1 - x)/x \quad (1)$$

where x is estimated by iterating the following term:

$$S/N = [1 - x/x]\ [-\ln(1 - x)] \quad (2)$$

where S is the number of species in the sample and N the total number of specimens. Jaccard's Similarity Index is used to compare faunal similarity between pairs of samples (here, stratigraphically adjacent samples):

$$Cj = C/S1 + S2 - C' \quad (3)$$

where C is the number of species common to both samples, and S1 and S2 are the total number of species in each sample. We used the Jaccard's Index to identify overall faunal similarity through the core sequences and times of rapid faunal overturn.

Carbon and oxygen isotopes were measured on samples of the widespread ostracode *L. lysandrosi*, which was abundant in most of the core samples (Palacios et al. 2016). Splits of *L. lysandrosi* were washed with high-purity DI water, sonicated to remove any adhering sediment, and dried at 50°C for four hours. For the analysis, we employed a Thermo Fisher Scientific GasBench II, equipped with a PAL autosampler, and coupled to a ConFlow IV interface and a MAT 253 mass spectrometer at the University of Utah. Samples were weighed using a Sartorious microbalance and loaded into Labco 4.5 ml flat-bottomed borosilicate vials and capped with butyl rubber septa. Each vial was flushed for six minutes on a PAL autosampler with ultra-high purity grade helium (99.999% He) at a flow rate of 50 mL/min. During flushing, vials were kept in a heated (75°C) aluminum block. The samples were reacted with ten droplets of 104% phosphoric acid at 75°C to evolve CO_2 gas and then allowed to equilibrate for four hours. Using the PAL autosampler, the produced CO_2 gas was collected using 100 microliter sampling loops and transported to the mass spectrometer. Nine individual injections were made for each sample and the reference materials; the average was taken to produce the values used on figures. For quality control, the standard deviation for carbon and oxygen isotopes were set at 0.2; if the standard deviation for any sample is higher than 0.2, the sample was re-analyzed. Three sets of reference materials were used to calibrate the system and unknown samples: (1) Carrara marble; (2) LSVEC; and (3) NBS-19. The Carrara marble and LSVEC standards were used as primary references,

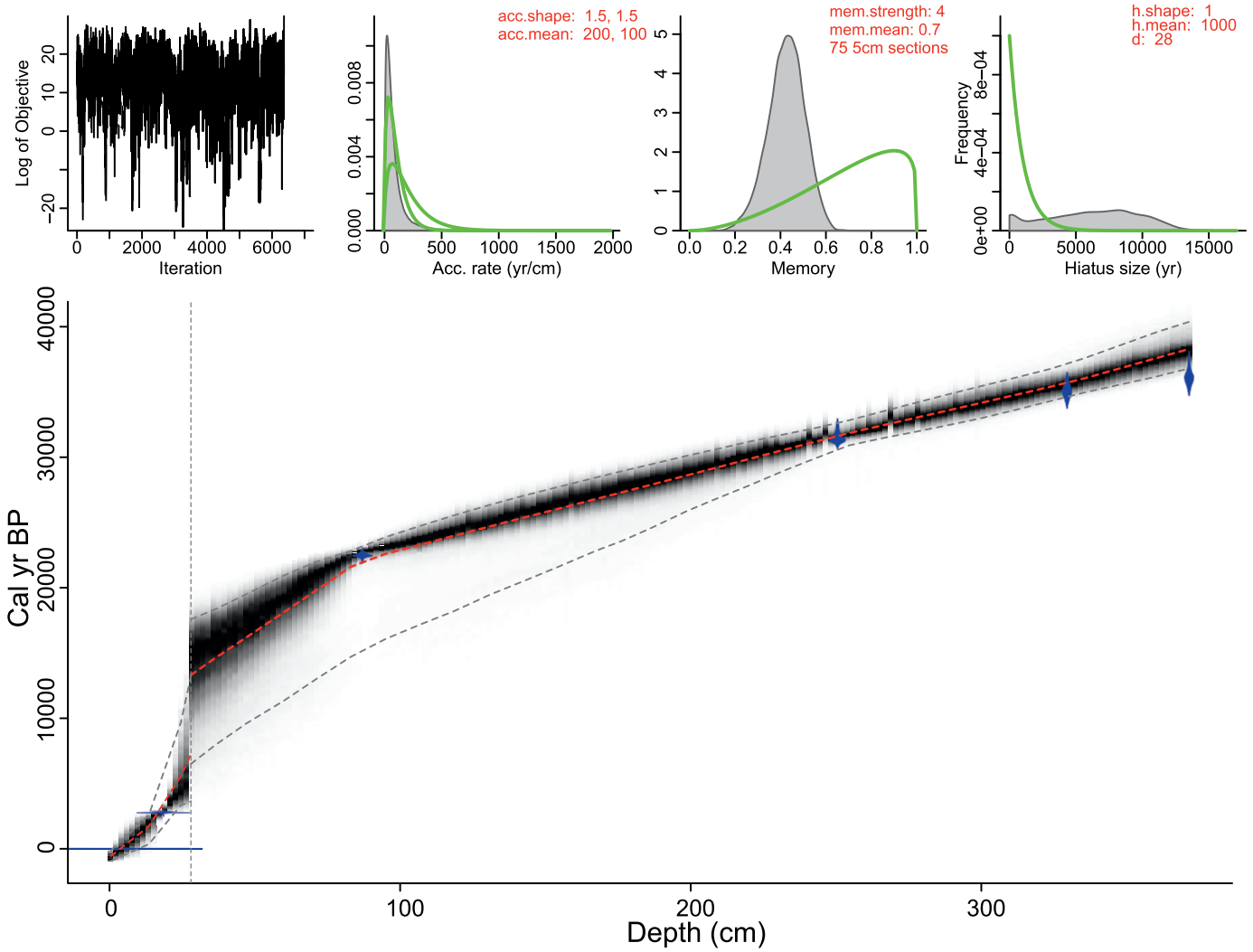

FIG. 4.—BACON-derived radiocarbon age model for core LP06-6A. Note the presence of an unconformity at ~ 28 cm below ground surface, which accounts for differences in sedimentation rates and depositional environments in the Holocene and late Pleistocene.

whereas the NSB-19 standard was used as secondary reference material to cross check the final result. The oxygen fractionation factor was calculated using the α value proposed by Kim et al. (2007). Isotope ratios are expressed in per mil notation relative to the PDB standard. Oxygen isotope values of ostracode carbonate should be dominantly influenced by the temperature and isotopic composition of ambient waters (Talbot 1990; Holmes 2008). Assuming no major changes in altitude or atmospheric precipitation sources at the PB in the late Quaternary, higher (lower) rates of evaporation and/or an increase (decrease) in temperature will drive values of $\delta^{18}O_{shell}$ higher (lower). The isotopic composition of dissolved inorganic carbon (DIC), as well as biological effects associated with carapace growth (vital effects), are dominant controls on $\delta^{13}C_{shell}$ values (Schwalb 2003; Leng and Marshall 2004).

Principal components analysis was conducted on normalized late Pleistocene–Holocene ostracode species assemblage and shell chemistry data using PAST version 3.16 (Hammer 2013). Two horizons in the dataset lacked stable isotope values, because *L. lysandrosi* valves were encrusted with carbonate that could not be removed. These missing values were accounted for in the dataset for using the iterative imputation function in PAST.

RESULTS AND INTERPRETATIONS

LP06-6A Age Model

BACON age-depth modeling for LP06-6A reveals that the hiatus at 28 cm below the lake floor omitted strata from ~13.3–7.2 ka (Fig. 4). Based on the mean of the modeled posterior distributions, average sedimentation rates from below the hiatus are 134 yrs/mm, and slower rates are observed above with an average of 222 yrs/mm when sedimentation resumes. Typically, a hiatus with no proximal dates would be difficult to constrain in time; this was a major limitation in the linear age-depth model presented in McGlue et al. (2013). However, the prior information about accumulation rates allows BACON to decide the most probable evolution and timing of the hiatus. Furthermore, it allows us to quantify age uncertainty at this interval. Modeled 95% confidence intervals suggest that age uncertainty is low from 40–20 ka as well as after the hiatus from 6 ka to modern. Around the hiatus, although the error cloud widens, MCMC runs do cluster most tightly around the weighted mean age depth model even at this interval. This suggests that even though uncertainty is greater around this depth, the ages of the hiatus top and bottom are reasonably well-constrained by the model despite the lack of absolute dates in this area.

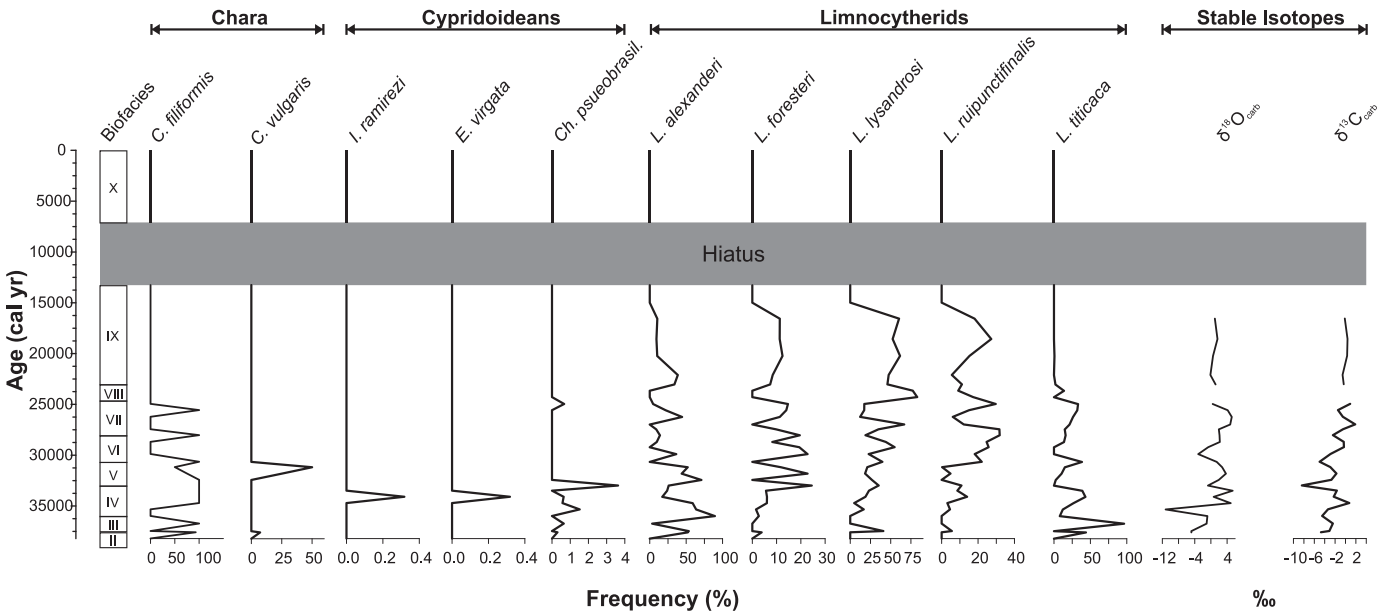

FIG. 5.—Integrated biofacies and shell chemistry for LP06-6A. Missing section, interpreted to have been removed by erosion during an interval of aridity, is marked by a gray box.

Biofacies

We adopted the ostracode taxonomy of Palacios-Fest et al. (2016) and defined biofacies in LP06-6A using patterns of species abundance, diversity, and taphonomy (see Online Supplemental File). Ostracode abundance varies greatly downcore and within the surface samples ($< 10^1$ to $> 10^4$ organisms/g), whereas the gyrogonites of *Chara* occur more sporadically within the lower portion of LP06-6A ($< 10^1$ organisms/g). Ostracode diversity and species richness is a hallmark of the late Quaternary at LP; two to eight species were found in each sample. Figure 5 summarizes LP's biostratigraphy and stable isotope chemostratigraphy.

Ostracodes of Extant LP.—Modern samples from Laguna de los Pozuelos contain an assemblage dominated by *L. foresteri*, *L. alexanderi*, and juveniles of *L. lysandrosi* (Fig. 3). *Limnocythere alexanderi* is abundant along the playa margins, whereas *L. foresteri* prevails in the playa lake center. *Chlamydotheca pseudobrasiliensis* rarely occurs in the playa margin and playa-lake center. At stations proximal to the Río Cincel delta, *I. ramirezi*, *L. foresteri*, and *L. lysandrosi* are common. *Limnocythere titicaca* is rare and was encountered in deltaic and eastern playa margin samples. Most modern stations contained four or five species; maximum diversity was encountered in station GB62, adjacent to the Río Cincel delta (Fig. 3). Fisher's α diversity index for modern samples averaged 0.64. Population density was highest in the offshore stations (> 5000 organisms/g) GB-60, GB-53, and GB-50.

We interpret the relatively well-preserved biological remains and complete individuals (carapaces with soft bodies inside) to reflect calm waters and capturing living forms in the modern deposystem. Low carapace fragmentation and abrasion suggest that the ostracode accumulations represent a biocenosis of the playa-lake. A near equal number of right and left valves, and adulthood (1:4 to 1:6) and disarticulation ratios (< 10 % carapaces) are consistent with this interpretation. Parts of the modern assemblage reflect more dilute hydrochemistry due to inflow from the Río Cincel, and we interpret that proximity to the delta helps to control ostracode species distributions, especially for species of cypridoideans, like *I. ramirezi* which thrives in flowing waters (Schwalb et al. 2002; Cusminsky et al. 2005). Ostracode diversity appears to be highest along the southeastern and eastern margins of LP, which is most likely linked to Río Cincel inflows and persistent standing water. Interestingly, a single gyrogonite of *Chara filiformis* was identified in GB-48, on the eastern playa margin (Fig. 4). The species lives in a wide range of environmental conditions with a high optimum pH (7.5–10.5; Romanov and Barinova 2012), which appears to demonstrate that salinity and alkalinity increase away from the southern axial deltas. However, a single specimen may not suffice to justify this interpretation.

Biofacies I (∼ 38.2–37.6 ka).—Biofacies I contained no ostracodes, and it characterizes the basal interbedded sands and diatom-rich silty clays in core LP06-6A.

We interpret this biofacies as deposits characterizing the basin during an episode of flooding and transgression that began prior to ∼ 38.2 ka. These sediments are coeval with a variety of green bedded sands and gravels, which were interpreted as medial to distal deltaic deposits by McGlue et al. (2013). The mineralogy of these deposits is consistent with a river source on the eastern flank of the PB, where Miocene-aged dacites and other volcanic deposits crop out.

Biofacies II (∼ 37.6–37.5 ka).—Biofacies II is dominated by *L. alexanderi*, with variable *L. titicaca* and *L. lysandrosi*, minor *L. foresteri*, and rare *Ch. pseudobrasiliensis*. Population density is low (< 950 organisms/g), as is diversity (three to four species), which is consistent with low Fisher's (< 0.51) index.

We interpret Biofacies II as a transitional environment during early transgression in the PB, which was probably marked by one or more shallow lakes or wetlands. Relatively little is known about this biofacies, as it is defined by only two samples in core LP06-6A. Lithofacies associated with this interval are massive green diatom ooze with elevated organic matter content, which McGlue et al. (2013) interpreted as lacustrine deposits under the influence of a delta.

Biofacies III (∼ 36.7–35.9 ka).—This biofacies consisted of *L. alexanderi* and *L. titicaca*, with the occasional appearances of *L. foresteri* and *Ch. pseudobrasiliensis*, especially near the base of the section. Population density is low (< 1000 organisms/g), as is diversity (three

species), which is consistent with low Fisher's (< 0.51) and steady Jaccard's (< 0.75) indices. Taphonomic data show low to moderately high fragmentation (10–40%) and low to moderately low abrasion (5–15%) of ostracode valves. A near even ratio of right to left valves, the 1:4 to 1:6 adulthood ratios, and the low number of carapaces (< 10%) distinguish the interval. Reduction stains were common. Intriguingly, *C. filiformis* reaches maximum values in Biofacies III.

We interpret the occurrence of calcareous algae to indicate a shallow lacustrine environment, which is consistent with the dark green massive silty clays that characterize the lithofacies containing these microfossils (McGlue et al. 2013). Lake water pH must have been higher than 8, however, in order to be consistent with the ostracode assemblage. The presence of gyrogonites and cypridoideans suggest that Biofacies III formed under the influence of deltaic inflow. Most of the valve breakage likely occurred due to post burial compaction, but reworking in a distal deltaic setting might also explain some of the damage.

Biofacies IV (~ 35.3–34.1 ka).—Biofacies IV consists of *L. alexanderi* and *L. titicaca*, with other limnocytherids present but rare. Cypridoideans occur occasionally in this interval, whereas gyrogonites from *C. filiformis* are rare. Ostracode population density is low to moderately high (700–3500 organisms/g), but diversity is the highest in the record with up to eight species present. Fragmentation is moderately high (> 30%) but abrasion remains low, implying that the most fragile valves broke during sample preparation. Low abrasion, however, indicates the organisms were not reworked but represented a local population, consistent with the 1:4 or 1:6 adulthood ratios.

We interpret the dense and diverse ostracode population to reflect a dilute and well-oxygenated perennial lake marked by deltaic inflows; the occurrence of calcareous algae also indicates shallow standing water. The presence of gyrogonites and cypridoideans suggest that Biofacies IV formed under the influence of deltaic inflow, and it bears some resemblance to the modern communities collected from stations adjacent to the Rio Cincel delta, especially GB-62.

Biofacies V (~ 33.5–30.7 ka).—*Limnocythere alexanderi* and *L. lysandrosi* dominate in Biofacies V, with minor occurrences of *L. foresteri*, *L. ruipunctifinalis*, and occasional appearances of *Ch. pseudobrasiliensis*. The highest population densities of ostracodes in LP06-6A occurred in this biofacies, with more than 7000 organisms/g, represented by up to five species. Fisher's index showed some variation throughout the section (0.35–0.71), whereas the Jaccard's index fluctuated from 0.63–1.00 within the unit. Valve damage patterns include moderate to very high fragmentation (20–70%) but low abrasion (< 2%), which suggests a local population with some potential for transport into the core site or post burial compaction. The near even ratio of right to left valves, the 1:4 to 1:6 adulthood ratios, and the low number of carapaces (< 10%) support a biocenosis interpretation for this biofacies. Gyrogonites from *C. vulgaris* and *C. filiformis* are present but rare in this interval.

Based upon the presence *Chara* and the dense ostracode population with abundant *L. alexanderi*, we interpret a shallow, alkaline, clear lacustrine environment for Biofacies V. The *Chara* prefer nearshore, transparent, and slow moving water less than 2 m deep, which is consistent with the dominant lithofacies (massive green silty clays) of this interval.

Biofacies VI (~ 30.0–28.7 ka).—Biofacies VI consists of a diverse ostracode fauna with *L. lysandrosi* and *L. ruipunctifinalis* as the dominant species. *Limnocythere alexanderi*, *L. foresteri*, and *L. titicaca* are present but less abundant, whereas cypridoideans and gyrogonites are absent. Ostracode population density reaches its lowest in the record (< 700 organisms/g) in spite of a variable species diversity. Fisher's index showed some variation (0.53–0.98) in contrast with the steady trend displayed by the Jaccard's index (1.00). The near even right to left valve ratio suggests a local population, but fragmentation and abrasion are relatively high (15–70% and 5–15%, respectively). Carbonate root casts and pyrite encrustations occur near the top of this facies, suggesting a well-oxygenated environment with little post-burial diagenesis.

We interpret the sharp decline in population density to indicate greater environmental stress in the basin, in association with prolonged dry seasons influencing a shallow saline wetland. This wetland biofacies correlates to Facies H of McGlue et al. (2013). The massive muds with abundant mottles recorded by those authors are consistent with root casts identified in this study, confirming a nearshore wetland setting marked by decaying macrophytes and extensive bioturbation. Facies H is also remarkable for its elevated concentrations of biogenic silica, which suggests that some organic or inorganic siliceous materials occurred in the wetland as well.

Biofacies VII (~ 28.0–25.0 ka).—Biofacies VII is dominated by *L. lysandrosi*, *L. ruipunctifinalis*, and *L. titicaca*, with minor *L. alexanderi* and *L. foresteri*. *Chara pseudobrasiliensis* occurs in the uppermost sample of the interval. Gyrogonites of *Chara filiformis* are rare at the base and top of this biofacies, which coincide with two episodes defined by the Jaccard's index (0.6–1.0) as a significant increase in species diversity. Population density remained low, with less than 2500 organisms/g. Fisher's index showed modest diversity variations (0.41–0.88), perhaps indicative of a highly variable environment. Valve fragmentation was variable (10–40%), but abrasion remained low (< 5%). With one exception, mineral coatings were low, but staining on some valves reflect reducing conditions. A near equal ratio of right to left valves, 1:4 to 1:6 adulthood ratios, and less than 10% disarticulation of carapaces suggest an autochthonous assemblage.

We interpret Biofacies VII to reflect benthic life in a saline lake that was influenced by dilute surface water. However, this lake had different characteristics than the saline lake represented by Biofacies III. Biofacies VII is marked by variable diversity and low population density, which we interpret to indicate greater hydrochemical instability. The presence of *Chara* and greater damage to ostracode carapaces suggest the possibility that the core site was in the proximity of a delta. Biofacies VII is incorporated within lower lithofacies D and upper lithofacies E (massive green silty clays) of McGlue et al. (2013). This demonstrates that the aquatic transition from saline lake to wetland was initially recorded in sediment composition, and only later reflected in the ostracodes and algae. This pattern suggests some resilience in *L. lysandrosi* and *L. ruipunctifinalis*.

Biofacies VIII (24.3–23.6 ka).—Biofacies VIII is one of the least diverse in the record, with *L. lysandrosi* dominant and at times nearly monospecific. *Limnocythere ruipunctifinalis* and *L. titicaca* were present in minor abundances, and gyrogonites were absent. Ostracode population density ranged from 691 to 2073 organisms/g. Fisher's index indicated wide variability (0.20–0.65) and Jaccard's index also varies significantly (0.33–1.00). Ostracode valves in Biofacies VIII were moderately fragmented (10–40%) and they exhibited low to moderate abrasion (< 15%). Carbonate or pyrite coated up to five percent of the valves. The biocenosis is formed by a rich suite of adults and juvenile valves (1:4 to 1:6 ratios), complete carapaces (< 10%), and a near equal right:left valves.

We interpret the depauperate ostracode population, taphonomic parameters, and mineral coatings as evidence for a saline wetland with fluctuating redox conditions. The biofacies characteristics are consistent with the pyrite-rich muds that dominate in this interval of the core (McGlue et al. 2013). The near monospecific assemblage reflects a harsh environment and provides evidence for the resilience and salinity tolerance of *L. lysandrosi*.

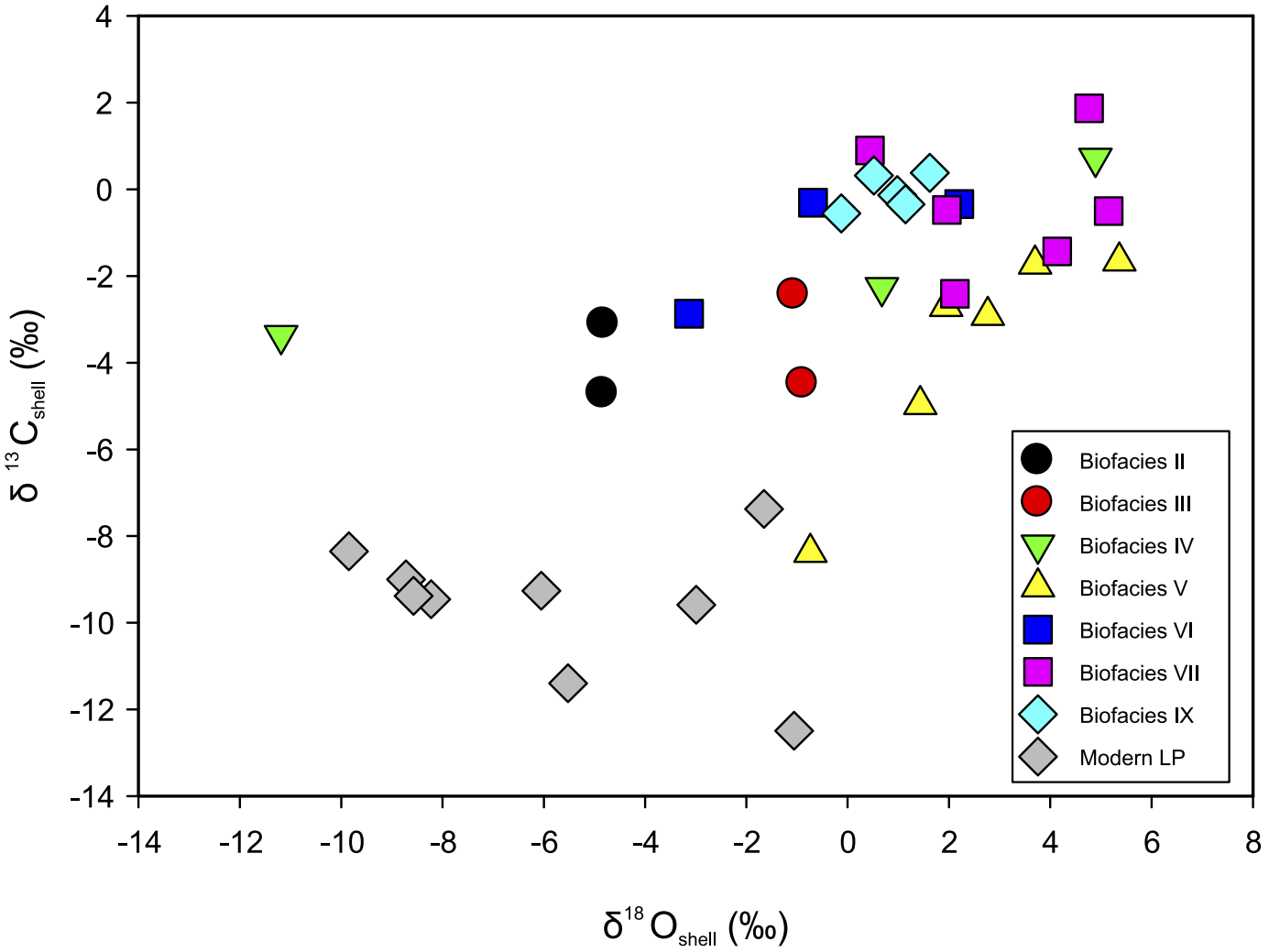

FIG. 6.—Cross plot of *L. lysandrosi* $\delta^{13}C_{shell}$ versus $\delta^{18}O_{shell}$. Ostracodes from Laguna de los Pozuelos show a broad range of $\delta^{18}O_{shell}$, likely reflecting differences in residence time of standing water and proximity to deltaic inflows. Ostracodes of Biofacies IX shows the narrowest range of isotope values, interpreted to be driven by the stability of a relatively large lake coeval with the Tauca phase paleolake elsewhere in the central Andes.

Biofacies IX (~ 23.0–13.3 ka).—Ostracodes were very abundant (> 5000 organisms/g) but not diverse in Biofacies IX, and calcareous algae were absent. *Limnocythere lysandrosi* was dominant and occurred with *L. ruipunctifinalis*, *L. alexanderi*, and *L. foresteri*. Valves were translucent and moderately fragmented (10–25%); abrasion and carbonate coatings were both very low (~ 2%). A near equal ratio of right to left valves, and the adulthood (1:4 to 1:6) and disarticulation ratios (< 10% carapaces) suggested a local population. Fisher's index showed modest variation among the samples (0.50–0.70), whereas Jaccard's index displays values greater than 0.80, indicating little change.

We interpret Biofacies IX to reflect a stable lacustrine environment from ~ 23.0 until at least 14.6 ka, where *L. lysandrosi* found the optimum conditions to establish a biocenosis. The high ostracode density but poor diversity are consistent with a saline lake occupying the basin. Taphonomic data suggest little diagenetic alteration. Biofacies IX occurs in Facies C of McGlue et al. (2013), which was inferred to reflect a dry mudflat environment on the basis of filled mudcracks, tilted silt laminae, minimal organic carbon, and very slow sedimentation rates. The combination of improved age modeling and the microfossil record allow us to re-interpret these sediments. Sedimentological evidence for lake desiccation and deflation are present, but only along the upper contact (~ 13.3 ka), which is consistent with the aquatic transition into Biofacies X.

Biofacies X (~ 7.2 ka–present).—No ostracodes or calcareous algae were recovered in these well-indurated clays following treatment with Glauber's salt and hot water. No biological remains were microscopically observed to be embedded in the sediments.

We interpret the paucity of benthic life in Biofacies X to be conditioned by an ephemeral playa-lake environment, marked by frequent subaerial exposure of the PB floor (McGlue et al. 2012). Neither persistent surface water inflows from the south, nor ephemeral floods from the Río Santa Catalina to the north, have had significant influence on benthic habitats at the LP06-6A core site since ~ 7.2 ka. Frequent subaerial exposure of the basin floor explains the density of these massive red clays (Facies A and the top of Facies C in McGlue et al. [2013]) and the scarcity of micro-crustaceans and green algae.

Stable Isotope Geochemistry

Modern.—Stable isotope values for modern *L. lysandrosi* are plotted on Figure 6. Modern ostracodes yielded $\delta^{18}O_{shell}$ values that ranged from -

9.9 to -1.1‰, with an average of -5.9‰. Corresponding $\delta^{13}C_{shell}$ values ranged from -12.5 to -7.4‰ and averaged -9.6‰. Although the dataset was relatively small, a spatial pattern was evident in the variable $\delta^{18}O_{shell}$ (Figs. 3, 6). *Limnocythere lysandrosi* collected from the eastern playa-lake margin (samples 46, 48, 50) were relatively ^{18}O-enriched, whereas ostracodes from the Río Cincel delta and western playa-lake were more depleted. We attribute more depleted $\delta^{18}O_{shell}$ from the southern basin axis and western margin to inflowing Río Cincel and Río Chico waters admixed with groundwater. Standing water is common in this area of the basin throughout much of the year, whereas the northern axis is much more susceptible to complete desiccation, due to the ephemeral nature of the Río Santa Catalina. Large swaths of the eastern margin of the playa-lake were also nearly desiccated from evaporation during our surface sediment sampling (McGlue et al. 2012). It follows that the shell isotopic composition of ostracodes living in this environment should have more positive $^{16}O/^{18}O$ ratios due to the effects of kinetic fractionation, which indeed they do (Fig. 6). Despite its closed surface hydrology, the modern playa-lake does not exhibit strong covariance between $\delta^{18}O_{shell}$ and $\delta^{13}C_{shell}$ ($r^2 = 0.10$).

Two online databases provide insights on the isotopic composition of modern precipitation in the Puna region. In general, the most negative $\delta^{18}O$ precipitation falls in the austral summer months (December, January, February, March) when monsoon rainfall arrives on the Puna and the amount effect couples with altitude to deplete ^{18}O (Clark and Fritz 1997). Station data from the IAEA-GNIP database (https://nucleus.iaea.org/wiser/) at Purmamarca (Argentina) and Tupiza (Bolivia) are most proximal to the PB, and show long-term $\delta^{18}O_{VSMOW}$ weighted means of approximately -6.6 +3.0‰ and -11.0 +0.3‰, respectively, whereas mean annual air temperature at those sites is 18.0 and 15.3°C. Similarly, the mean annual $\delta^{18}O_{VSMOW}$ from the Waterisotopes.org web archive at the PB is -10.2‰ (e.g., Bowen and Revenaugh 2003). Using the transfer functions of Hren and Sheldon (2012), a conservative predicted range for Laguna de los Pozuelos surface water temperature is ~ 16–23°C. Interestingly, the average $\delta^{18}O_{VPDB}$ of ostracodes collected from standing water in the playa-lake is -5.9‰ ($n = 9$), whereas empirically predicted $\delta^{18}O_{VPDB}$ of calcite crystallized from rainfall-derived surface water in the Puna is ~ 1.3–10.5‰, assuming the full range of isotope values from the IAEA and Waterisotopes.org databases. The considerable per mil differences between the $\delta^{18}O_{VPDB}$ of modern ostracodes and calcite from precipitation assuming equilibrium fractionation must reflect groundwater mixing and residence time within Pozuelos basin aquifers. Additional study is needed to clarify the causes of depleted modern shell $\delta^{18}O$ from Pozuelos, but the marked difference between modern and ancient shell $\delta^{18}O$ appears to capture the hydrological transition from the late Pleistocene glacial and deglacial into the late Holocene, which is strongly reflected in ostracode abundance and diversity.

Ancient.—Most of the chemostratigraphic variability in ostracode $\delta^{18}O_{shell}$ and $\delta^{13}C_{shell}$ was found within Biofacies II through VII (Fig. 5). Biofacies II, III and the deepest sample from Biofacies IV $\delta^{18}O_{shell}$ were the most negative in the dataset (average = -4.6‰, n = 5), and carbon isotope values from these samples were also uniformly negative (average = -3.6‰) with a relatively narrow absolute range (-4.7 to -2.4‰). A progressive trend toward larger $\delta^{18}O_{shell}$ values marked the transition from upper Biofacies IV into Biofacies V (average = 2.5‰, n = 8). More variability was apparent in $\delta^{13}C_{shell}$ through these facies (-8.4 to 0.7‰), but the average was similar to the underlying shells (~ -3.0‰). Together, oxygen and carbon isotope values in Biofacies V exhibit a strong positive correlation ($r = 0.83$, $p < 0.02$); Biofacies V is unique in the record in the strength of its $\delta^{18}O_{shell}$ and $\delta^{13}C_{shell}$ covariance. Biofacies VI also shows a progressive trend towards more positive $\delta^{18}O_{shell}$ through time (average = -0.5‰; $n = 3$), while $\delta^{13}C_{shell}$ displays a narrow range of variability (-2.9 to -0.3‰; average = -1.2‰). Oxygen and carbon isotopes still show a relatively strong correlation ($r = 0.69$, $p < 0.02$). In Biofacies VII, $\delta^{18}O_{shell}$ and $\delta^{13}C_{shell}$ shifted towards more positive values (average = 3.1‰ and -0.34‰, respectively). The overlying Biofacies IX was characterized by relative isotopic stability and high average $\delta^{13}C_{shell}$ (~ -0.1‰; Fig. 6). *Limnocythere lysandrosi* from Biofacies IX were relatively enriched in ^{18}O (average = ~0.8‰), though values were several per mil more negative than the underlying Biofacies VII.

Depleted ostracode $\delta^{18}O_{shell}$ from Biofacies II, III, and the base of IV are consistent with carapace growth in relatively dilute lake water, perhaps owing to proximity to a stream inlet. The presence of *I. ramirezi* in the species assemblage appears to confirm a deltaic influence. By contrast, covariant $\delta^{18}O_{shell}$ and $\delta^{13}C_{shell}$ exhibited in Biofacies V suggest a much stronger influence of evaporation at that time. Talbot (1990) observed covariance between $\delta^{18}O_{shell}$ and $\delta^{13}C_{shell}$ measured on carbonates from hydrologically closed lakes. Biofacies VII is the most enriched in ^{18}O, which is consistent with the depositional environment interpretation of a saline wetland marked by a short residence time of standing water. Although interpretation of $\delta^{13}C_{shell}$ are less certain as they are subject to influences from more factors, relatively positive values may reflect changes to DIC composition influenced by redox chemistry and organic matter decomposition. The narrow range of $\delta^{18}O_{shell}$ in Biofacies IX, as well as low covariation with $\delta^{13}C_{shell}$ ($r^2 = 0.31$), could potentially signify a hydrologically open lake (Cohen 2003). The oxidized tan massive muds with low organic matter content from which Biofacies IX ostracodes were recovered provide few insights on water levels, due to post depositional alteration by subaerial exposure and oxidation (McGlue et al. 2013). However, the absence of paleoshorelines along the basin spill point elevation indicates that the basin was most likely maintained surficial hydrological closure. Therefore, we interpret this pattern of isotopic compositions to reflect a relatively large and stable hydrologically closed lake.

DISCUSSION

Ostracode Paleoecological Records in the Pozuelos Basin

Ostracode records have been produced for many Quaternary studies, but relatively few examples exist that use these microcrustaceans to infer aspects of water balance and chemistry in South America (Schwalb et al. 1999; Whatley and Cusminsky 1999; Cusminksy et al. 2011; Mercau et al. 2012; Laprida et al. 2015; Ramos et al. 2016). Schwalb et al. (2002) demonstrated that ostracode assemblages and shell chemistry could successfully be used to identify three different types of paleoenvironments: (1) springs, seeps, and streams; (2) permanent ponds and lakes; and (3) ephemeral ponds and lakes. The existing late Quaternary paleogeographic framework for the PB suggests that depositional environments changed dramatically in the basin, with a seasonal playa-lake with axial rivers marking the late Holocene (~ 3.0 ka–present), a much larger but variable lake fed by a lateral river system in the late Pleistocene (~ 42.0–19.0 ka), and a deflated or reworked interval separating the two different hydrologic phases (~ 19.0–3.0 ka) (McGlue et al. 2013). Lithofacies and preservation of organic carbon suggested that although depositional environments varied, the basin was persistently hydrologically closed (McGlue et al. 2013). The biofacies and age modeling presented here allow us to critically evaluate and refine these paleoenvironmental interpretations, and at the same time enable a more rigorously constrained comparison with key Quaternary geological archives from the region.

New biofacies data show that ephemeral aquatic ecosystems dominated over the past ~ 38.0 kyr in the PB, with periodic transitions to more permanent and deeper lake conditions. The hydrochemistry of modern LP is marked by Na^+, Cl^-, and SO_4^{2-} in a HCO_3^--enriched system (McGlue et al. 2012). Faunal assemblages imply that these ions fluctuated widely during the late Pleistocene and Holocene, with more diverse and abundant

ostracodes during stable lake phases, and less diverse assemblages characterized the PB when hydrochemistry was more variable in ephemeral saline wetland phases. *Limnocythere lysandrosi*, *L. ruipunctifinalis*, and *L. alexanderi* are the three most consistent species throughout the fossil record, implying eurytopic characteristics such as the tolerance of a wide salinity range. It was for this reason that carbon and oxygen stable isotope measurements were made on *L. lysandrosi*. *Limnocythere titicaca* by contrast may be amongst the most vulnerable to salinity variations, as the species are restricted to more dilute surface waters (Mourguiart and Corrége 1998).

Lake Phases

Three saline lake phases occurred in the PB. The older lake phase lasted from ~ 37.6–30.7 ka, which partially overlaps the well-known but sometimes disputed Minchin Pluvial on the Altiplano (Placzek et al. 2006; Fritz et al. 2007). This lake phase is coincident with Biofacies II through V; *Chara* biomass suggests that alkalinity was relatively high (pH > 8) but variable. Lithofacies associated with this lake phase include organic matter rich laminated muds and massive green silty clays, which are consistent with sublacustrine deposition by suspension settling (McGlue et al. 2013). Occurrence of *Ch. pseudobrasiliensis* in these biofacies supports the hypothesis of a deltaic influence nearby, as the genus *Chlamydotheca* prefers lentic ecosystems with abundant vegetation (Torres and Martinez 2010). A short lake phase occurred at ~ 28.0–25.0 ka, represented by Biofacies VII. This humid interval preceded the Last Glacial Maximum (LGM), and was marked by a shallow but positive water balance in the Salar de Atacama, and by a variable gamma response in Uyuni basin strata, indicating mud deposition and fluctuating lake level (Bobst et al. 2001; Fritz et al. 2004). Massive green silty clays mark this phase, which are a common shallow, well-oxygenated lake facies (Cohen 2003). Basin margin strata examined by Camacho et al. (2014) found that PB experienced a lake expansion between > 43 and 23 ka, which at its maximum reached ~ 900 km^2 but commonly fluctuated to below ~ 600 km^2.

Climatic and tectonic events at the end of the LGM generated a younger lake phase (~ 23.0–14.6 ka) reflected in Biofacies IX. LP lithofacies and biofacies overlap the shallow Sajsi lake phase and the Tauca Pluvial observed across the central Andes (e.g., Baker et al. 2001a; 2001b; Placzek et al. 2006). The lithofacies associated with this lake is a massive tan mud with a paucity of organic matter and biogenic silica (McGlue et al. 2013). Oxidation and desiccation features at the top of strata hosting Biofacies IX suggest that the lake underwent a severe contraction following deposition of this unit, as climate became much drier. We interpret that this episode of aridity spurred erosion of basin floor lake strata, most likely by deflation.

Wetland Phases

Two shallow wetland phases occurred in the PB, at ~ 30.0–28.7 ka and ~ 24.3–23.6 ka. These saline wetlands are represented by Biofacies VI and VIII, respectively. Low ostracode population densities and poor diversity indicate a relatively harsh environment for benthic life. Lithofacies associated with the wetlands include mottled green-brown clays with root casts and black pyritic muds (McGlue et al. 2013). Both wetland biofacies capture the environments that followed lake contraction, when the basin floor was most likely evaporative and partially covered with shallow, stagnant, dysoxic water.

Playa-Lake Phase

Extant LP has no analog in the late Pleistocene history of the PB, and our chronology suggests this ephemeral playa-lake system developed after ~ 7.2 cal ka. Camacho et al. (2014) estimated that PB continued to contract to ~ 264 km^2 at the late Pleistocene–Holocene transition and more drastically to ~ 112 km^2 during the early Holocene, which is consistent with our age model estimation of the core hiatus boundaries. Notably, southern hemisphere insolation was low at tropical latitudes in the mid-Holocene, which may explain the dramatic transition in PB hydrology and depositional environments (Fig. 7). In contrast with lake and wetland phases, the large swaths of the ephemeral playa fully desiccate and remain without water for many months of the year, which strongly influences the composition of sediment accumulating in the PB (McGlue et al. 2012). Ostracodes and *Chara* are most abundant in the southern axis of the basin, where strong annual Río Cincel baseflow has a pronounced impact, and in areas with groundwater discharge along the flanks of the basin floor (Igarzabal 1978).

Regional Integration

Because of their sensitivity to changes in effective precipitation (Teller and Last 1990), extant closed-basin lakes like LP hold the potential to provide useful data on environmental dynamics in the Andes. Late Quaternary Andean paleoclimate has been vigorously debated, mostly due to inconsistencies in geochronology since the geological evidence (e.g., bathtub ring-like paleo-shorelines) for variability in water balance is largely unequivocal (Placzek et al. 2013; Baker and Fritz 2015). Without robust dating, interpretations about the atmospheric controls driving paleohydrology were subject to controversy.

Perhaps the most important aspect of the present study was to clarify the nature and timing of late Pleistocene and Holocene aquatic transitions in the PB, which will shed light on the relative influence of climate and tectonics. We improved upon the linear age modeling of McGlue et al. (2013) by using BACON and sedimentological characteristics of core LP06-6A, which permitted a more accurate estimation of a hiatus that omitted ~ 6.1 kyrs of section from ~ 13.3–7.2 ka. The best explanation for this feature is low Southern Hemisphere summer insolation, which severely reduced monsoon rainfall in the early Holocene (e.g., Baker et al. 2001a; Baker and Fritz 2015) (Fig. 7). Better constraints on this hiatus afforded the new opportunity to interpret glacial and interglacial patterns of biofacies development in conjunction with previously published lithofacies data (McGlue et al. 2013). The use of linear age modeling required an extended interval of reworking and slow sedimentation rates from ~ 19.0–3.0 ka, which appeared consistent with the highly oxidized, organic matter poor muds from this interval. However, this interpretation must be reconsidered in light of new biofacies data. The abundance of limnocytherids sharply declines at the top of Biofacies IX, consistent with a regression and subaerial exposure of the basin floor. This hiatus-producing event appears to have oxidized the underlying muds, which obscured the interpretation of depositional environment. This penetration of an oxidation front is not unusual for organic-rich fine-grained rocks, however. Petsch et al. (2000) observed that weathering rinds on mudrocks can range up to several meters thick, and the total organic carbon content of these altered muds do not faithfully record the original depositional signal. The biofacies make clear that these sediments were deposited in a persistent saline lake, very much in accord with other basins in the region that experienced lake level highstands associated with the Tauca phase.

We interpret the first principal component in our analysis (PC1; 29% of variance explained) of ostracode species assemblages and shell chemistry as an indicator of deltaic inflows (Fig. 7). For PC1, loadings are positive for *L. lsyandrosi*, *L. ruipunctifinalis*, $\delta^{18}O_{shell}$, and $\delta^{13}C_{shell}$ and suggest an absence of strong deltaic influence. By contrast, loadings are strongly negative for *L. titicaca*, *L. alexanderi*, and the cypridoidean species, indicating the influence of inflowing water to the core site. Figure 7 places PB ostracode and *Chara* abundances, as well as PC1 in context with regional keystone paleoclimate records from the Salar de Uyuni, the Salar de Atacama, and Lake Titicaca, as well as an insolation curve for 20°S. The PC1 values from ~ 37.6–29.9 ka suggest the presence of a delta. Strata at

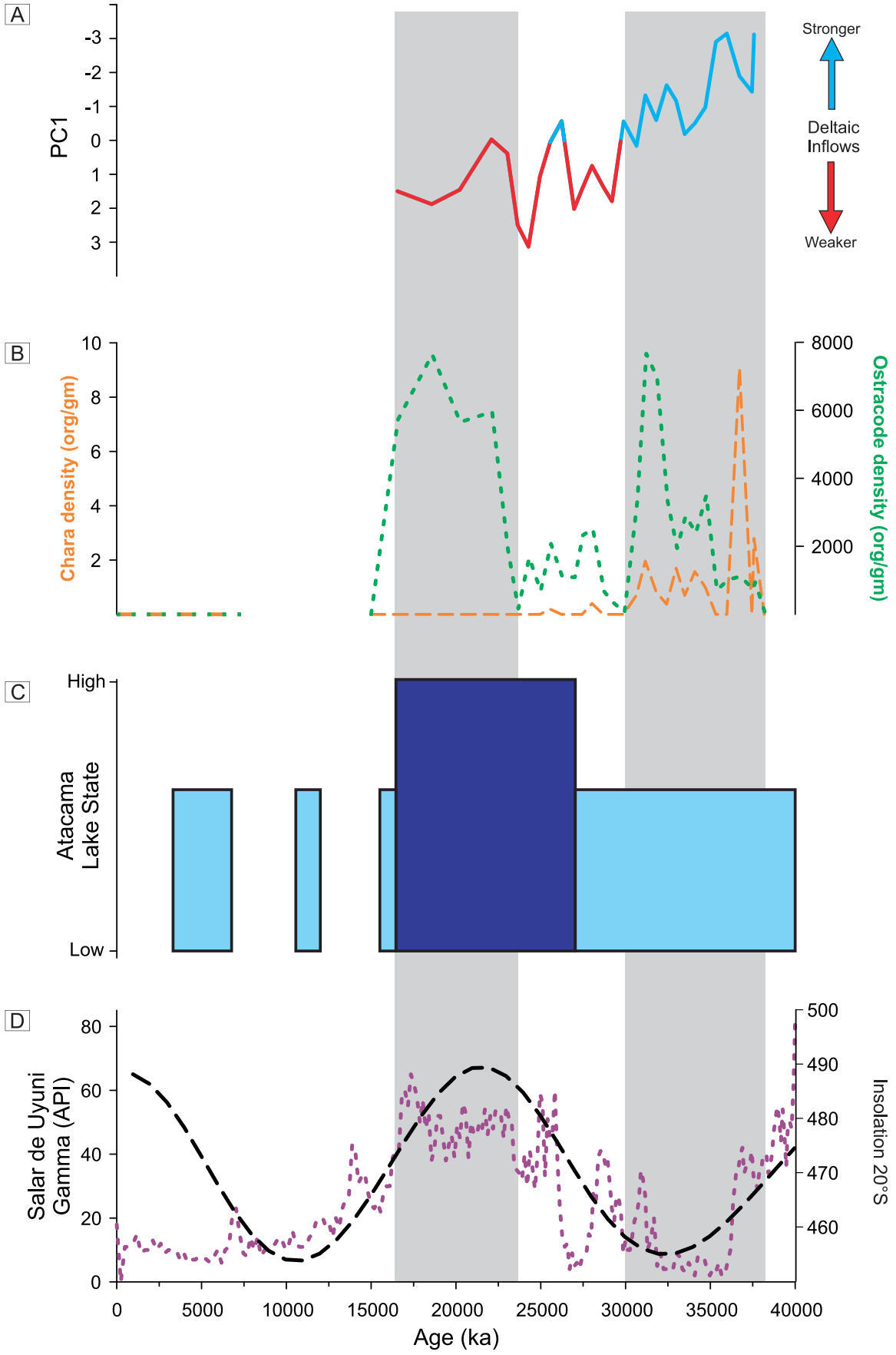

FIG. 7.—Synthesis of Pozuelos Basin ostracode paleoecology with paleoenvironmental records from the central Andes. **A**) Ostracode PC1 derived from LP06-6A. Note that scale is reversed. **B**) Ostracode (green) and Chara (orange) biomass from LP06-6A. **C**) Atacama lake stage (modified from Bobst et al. 2001). Dark blue shading represents deep lake phases, whereas light blue depicts intervals with shallow aquatic environments. **D**) Salar de Uyuni drill core gamma ray log (modified from Fritz et al. 2007) and January insolation curve for 20°S (from Berger 1978; Berger and Loutre 1991).

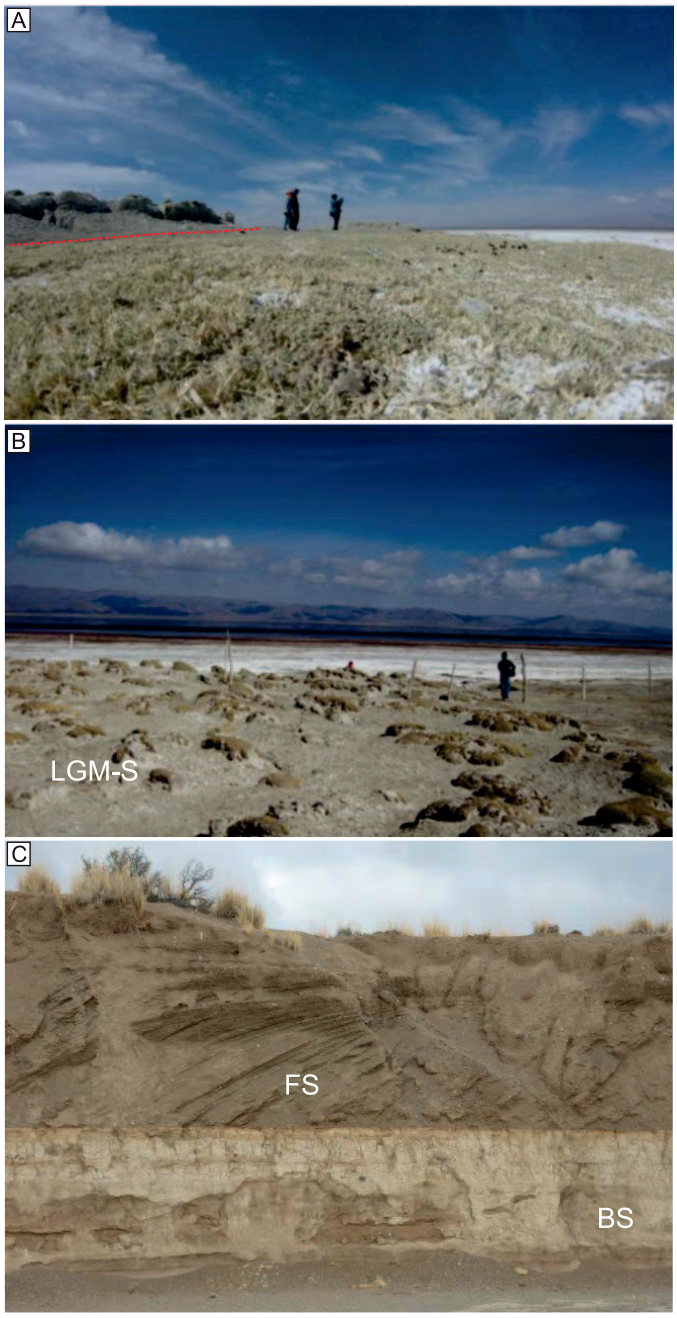

FIG. 8.—Field photos of normal fault trace (A) and LGM shoreline (LGM-S) (B) on the eastern margin of the Pozuelos Basin (*cf* Camacho and Kunz 2013). Photo (C) illustrates Gilbert-style deltaic foresets (FS) and bottomset (BS) beds discovered near the Arroyo Corral Blanco, which has been deformed by a normal fault inferred to run along much of the eastern playa-lake shore. Outcrop is approximately 4.3 m from base to top. See text for details.

this interval are comprised by Biofacies II through the base of Biofacies VI; comparisons with modern ostracodes living adjacent to the Río Cincel delta suggest that inflows may have been strongest in Biofacies IV. Prior research documented basal green deltaic sands and gravels in four broadly distributed sediment cores from northern LP, which suggested that: (1) the river supplying the delta drained Tertiary dacites on the eastern flank of the basin; (2) the delta complex had prograded into a position presently occupied by the axis of LP; and (3) the delta system was established by at least ~ 42.0 ka (McGlue et al. 2013). A study by Camacho and Kunz (2011) documented the presence of upward-coarsening deltaic lobes in outcrops on the northeastern margin of the PB (Fig. 8). These strata consist of brown sands and gravels, thus it remains unknown if the influence of this delta solely influenced biofacies at the LP06-6A core site, or if another lateral delta(s) also played a role. Nevertheless, documentation of deltaic lobes by Camacho and Kunz (2011) provides compelling evidence for the existence of west and southwest flowing rivers in the surface hydrologic network of the basin in the late Pleistocene. Those authors used ^{14}C to date deltaic deposits to ~ 28.5–18.0 ka. At the LP06-6A site, the transition to the saline wetland marked by Biofacies VII at ~ 24.3 ka BP appears to be the last instance when the center of LP was routinely influenced by deltaic inflows, which we interpret to be a result of both climatic and tectonic change. Water levels dropped at the core site in Biofacies VIII (24.3–23.6 ka); this ~ 700 yr period was probably characterized by reduced runoff to the lake during a transient arid interval. As water levels rose with increased monsoon rainfall during Biofacies IX, we interpret that any deltaic systems debouching into the lake stepped backward towards the basin margin. The absence of a strong deltaic signal in our PC1 at this time is consistent with lake expansion and migration of the shoreline away from the core site, which allowed an offshore ostracode assemblage to thrive.

Camacho and Bossi (2013) showed that the mouth of the Arroyo Corral Blanco, a candidate feeder channel for one lateral paleo-delta, was dissected by a normal fault that became active ~ 18.2 ka (Figs. 1, 8). The timing of this fault movement pre-dates the intact strata at the top of Biofacies IX at ~ 14.6 ka, which indicates that tectonic modification of lateral deltaic trunk and distributary channels may have been a threshold that contributed to a major aquatic transition that transformed the PB. Following this model, fault-related channel dissection and delta collapse reorganized the surface water drainage network. This occurred just before a significant decline in insolation at 20°S and summer monsoon rainfall at the end of the Tauca phase at ~ 15 ka. If tectonic alteration of the river network reduced the amount of water delivered to delta mouths, overall lake volume may have declined as well. This effect is particularly acute in flat floored basins that lack deeply subsided depocenters. As the monsoon began to fail, the lake of Biofacies IX likely contracted sharply, but evidence of this regression, as well as any subsequent lake level rise associated with a Coipasa-aged pluvial (~ 13.0–11.0 ka; Placzeck et al. 2006), is absent from our core due to the unconformity between Biofacies IX and X. Using onshore stratal records (paleosols), Camacho et al. (2014) showed a pronounced episode of lake contraction was registered around 12 ka ^{14}C BP (~ 14–13.7 ka). Early Holocene aridity, again linked to a reduction of southern hemisphere insolation, was implicated by McGlue et al. (2013) to explain desiccation features at the top of Biofacies IX deposits, and the present study appears to confirm an important role for orbital controls on monsoon rainfall in the PB. A similar early Holocene aridity signal was registered at the endorheic Guayatayoc-Salinas Grandes depression, located < 100 km south of the Pozuelos Basin (Lopez Steinmetz and Galli 2015). When insolation began to recover in the middle Holocene, the lentic ecosystem that developed at LP was the shallow playa-lake that we know today, which is hydrologically dominated by the rivers entering the basin from the south and groundwater discharge.

CONCLUSIONS

The high altitude Pozuelos Basin is a flat-floored, endorheic hinterland transitional basin on the Puna Plateau of northwest Argentina. This basin type has only recently been recognized, due to the new appreciation for cyclic magmatic processes influencing basins associated with Cordilleran orogenic systems (DeCelles et al. 2009). The Pozuelos Basin is bounded by westward-vergent thrust faults, but neotectonic deformation is dominated by normal faulting, which appears to have influenced Quaternary hydrology and depositional

patterns in the basin. At the center of the basin sits LP, a large and shallow playa-lake that is important to Andean biodiversity and endemism. We used calcareous microfossils recovered from a lake sediment core and modern sediment samples to improve our understanding of the stratigraphy and paleohydrology of the basin since ~ 38.3 ka. Ten ostracode biofacies were defined in the core; species assemblages and shell chemistry downcore were compared to modern samples to inform our interpretations. Integration of biofacies data with lithostratigraphy improved our understanding of the stratal completeness of LP, and allowed us to refine the radiocarbon age model and constrain the missing time associated with an unconformity at the Pleistocene–Holocene transition to ~ 6.1 kyrs. The presence of an erosional gap from ~ 13.3–7.2 ka is consistent with aridity and subaerial exposure of the basin floor when summer insolation and monsoon rainfall declined in the southern hemisphere tropics during the early Holocene.

Variability in paleohydrology exerted the strongest influence on biofacies and the isotopic composition of ostracode shell carbonate. A pronounced change in the surface water hydrologic network was the cessation of one or more lateral deltas that built into the basin from the east margin. Inflow from these rivers influenced aquatic habitats and benthic fauna at the core site, whereas the modern Río Cincel delta (southern axis) and Río Santa Catalina terminal splay (northern axis) appear to have little effect on depositional environments in the center of LP. Clear evidence exists for the collapse of one delta on the eastern margin at ~ 18.2 ka, driven by normal faulting. Ostracodes and *Chara* appear to confirm the persistence of hydrologic closure in the PB throughout the latest Quaternary. An expansive lake phase with depleted $\delta^{18}O_{shell}$ occurred from ~ 37.6–30.7 ka, but available sedimentary and paleoecological evidence indicates that water levels probably remained below the basin sill. Ostracode population densities indicate that the late Pleistocene was subjected to the expansion of a relatively large saline lake from ~ 23.0–16.1 ka, which overlaps in time with the Tauca highstand, a pluvial event that has been identified in a number of paleo-records from the central Andes. Isotope data suggest this lake could have been hydrologically open, but facies characteristics and the absence of prominent paleo-shorelines indicate that water levels most likely remained below the PB spill point. Transitions in aquatic environments, particularly after ~ 30.6 ka, appear to have been more gradual than abrupt. Wetland phases, most likely supported by groundwater discharge, exhibited only minor differences in species assemblages and the isotopic composition of *L. lysandrosi* from ~ 30.6–22.0 ka. Finally, the character of depositional environments observed in the basin today appears to have been established no earlier than the mid-Holocene.

ACKNOWLEDGMENTS

We are grateful to NSF (EAR-0542993), ACS/PRF (45910-AC8), CONICET PIP 00021; MINCYT PICT 2014-1271, and ExxonMobil Upstream Research for their financial support of this research. A. Cohen, J. Omarini, L. Lupo, R.G. Cortes, A. Kirschbaum, and the staff of staff of PN Laguna de los Pozuelos are thanked for their assistance with this research. The staff of LacCore graciously assisted with all aspects of core processing, archival, and sampling. F.R. Gío-Argáez and A.L. Carreño, as well as Y. Hornelas, M. Berenit Mendoza-Garfias and B. Martínez from the National Autonomous University of Mexico, and W. Waldrip from the University of Arizona assisted us with the scanning electron microscope imagery. We thank the PALAIOS editors and reviewers for their comments on an earlier version of the manuscript.

SUPPLEMENTAL MATERIAL

Data are available from the PALAIOS Data Archive: http://www.sepm.org/pages.aspx?pageid=332.

REFERENCES

Alonso, R.N., Jordan, T.E., Tabbutt, K.T. and Vandervoort, D.S., 1991, Giant evaporite belts of the Neogene Central Andes: Geology, v. 19, p. 401–404.

Anadón, P., Utrilla, R., and Vázquez, A., 2000, Use of charophyte carbonates as proxy indicators of subtle hydrological and chemical changes in marl lakes: example from the Miocene Bicorb Basin, eastern Spain: Sedimentary Geology, v. 133, p. 325–347.

Apolinarska, K. and Hammarlund, D., 2009. Multi-component stable isotope records from late Weichselian and early Holocene lake sediments at Imiołki, Poland: palaeoclimatic and methodological implications: Journal of Quaternary Science, v. 24, p. 948–959.

Baker, P.A. and Fritz, S.C., 2015, Nature and causes of Quaternary climate variation of tropical South America: Quaternary Science Reviews, v. 124, p. 31–47.

Baker, P., Rigsby, C., Seltzer, G., Fritz, S., Lowenstein, T., Bacher, N., and Veliz, C., 2001b, Tropical climate changes at millennial and orbital timescales on the Bolivian Altiplano: Nature, v. 409, p. 698–701.

Baker, P., Seltzer, G., Fritz, S., Dunbar, R., Grove, M., Tapia, P., Cross, S., Rowe, H., and Broda, J., 2001a, The history of South American tropical precipitation for the past 25,000 years: Science, v. 291, p. 640–643.

Berger, A., 1978, Long-term variations of daily insolation and Quaternary climatic changes: Journal of Atmospheric Science, v. 35, p. 2362–2367.

Berger A. and Loutre, M.F., 1991, Insolation values for the climate of the last 10 million years: Quaternary Science Reviews, v. 10, p. 297–317.

Blaauw, M. and Christen, J.A., 2011, Flexible paleoclimate age-depth models using an autoregressive gamma process: Bayesian Analysis, v. 6, p. 457–474.

Bobst, A.L., Lowenstein, T.K., Jordan, T.E., Godfrey, L.V., Ku, T.L., and Luo, S., 2001, A 106 ka paleoclimate record from drill core of the Salar de Atacama, northern Chile: Palaeogeography, Palaeoclimatology, Palaeoecology, v.173, p. 21–42.

Bowen, G.J. and Revenaugh, J., 2003, Interpolating the isotopic composition of modern meteoric precipitation: Water Resources Research, v. 39, p. 1299, doi:10.1029/2003WR002086.

Brouwers, E.M., 1988, Sediment transport detected from the analysis of ostracod population structure: an example from the Alaskan Continental Shelf, *in* P. De Deckker, J.-P. Colin, and J.-P Peypouquet (eds.), Ostracoda in the Earth Sciences: Elsevier, Amsterdam, The Netherlands, p. 231–244.

Caffe, P.J., Trumbull, R.B., Coira, B.L., and Romer, R.L., 2002, Petrogenesis of early Neogene magmatism in the Northern Puna; implications for magma genesis and crustal processes in the Central Andean Plateau: Journal of Petrology, v. 43, p. 907–942.

Camacho, M. and Bossi G.E., 2013, Desarrollo de delta "Tipo Gilbert" transversal, durante el Pleistoceno tardío, en una cuenca lacustre de la Puna jujeña: Investigaciones en Facultades de Ingeniería del NOA, Santiago del Estero, CD ROM 13.

Camacho, M. and Kunz, A., 2011, Sedimentos del testigo de la perforación al NE de La Laguna de Los Pozuelos Actual, Puna jujeña, Argentina: Investigaciones en Facultades de Ingeniería del NOA, San Fernando del Valle de Catamarca, v. 1, p. 375–382.

Camacho, M., Visich, M.C., and Kulemeyer, J.J., 2014, Estudio del Cuaternario Tardio en las Cuencas de la Laguna de los Pozuelos y Salinas Grandes-Guayatayoc, Puna Argentina: XIX Congreso Geologico Argentino, Cordoba.

Cladouhos, T.T., Allmendinger, R.W., Coira, B. and Farrar, E., 1994, Late Cenozoic deformation in the Central Andes: fault kinematics from the northern Puna, northwestern Argentina and southwestern Bolivia: Journal of South American Earth Science, v. 7, p. 209–228.

Clark, I.D. and Fritz, P., 1997, Environmental isotopes in hydrogeology: CRC Press, Boca Raton, 342 p.

Cohen, A.S., 2003, Paleolimnology: the History and Evolution of Lake Systems: Oxford University Press, New York City, 500 p.

Cohen, A., McGlue, M.M., Ellis, G.S., Zani, H., Swarzenski, P.W., Assine, M.L. and Silva, A., 2014, Lake formation, characteristics, and evolution in retroarc deposystems: a synthesis of the modern Andean orogen and its associated basins, geodynamics of a Cordilleran Orogenic System: the Central Andes of Argentina and Northern Chile: Geological Society of America Memoir, v. 212, p. MWR212–216, doi: 10.1130/2015.1212(16).

Cusminsky, G.C., Pérez, P.A., Schwalb, A., and Whatley, R.C., 2005, Recent lacustrine ostracods from Patagonia, Argentina: Revista Española de Micropaleontología, v. 37, p. 431–450.

Cusminsky, G.C., Schwalb, A., Pérez, A.P., Pineda, D., Viehberg, F., Whatley, R., Markgraf, V., Gilli, A., Ariztegui, A., and Anselmetti, F.S., 2011, Late Quaternary environmental changes in Patagonia as inferred from lacustrine fósil and extant ostracodes: Biological Journal of the Linnean Society, v. 103, p. 397–408.

D'Agostino, K., Seltzer, G.O., Baker, P., Fritz, S.C. and Dunbar, R., 2002, Late-Quaternary lowstands of Lake Titicaca: evidence from high-resolution seismic data: Palaeogeography, Palaeoclimatology, Palaeoecology, v. 179, p. 97–111.

DeCelles, P.G., Carrapa, B., Horton, B.K., McNabb, J., Gehrels, G.E., and Boyd, J., 2014, The Miocene Arizaro Basin, Central Andean Hinterland: response to partial lithosphere removal?: Geological Society Of America Memoirs, v. 212, p. 359–386.

DeCelles, P.G., Ducea, M.N., Kapp, P., and Zandt, G., 2009, Cyclicity in Cordilleran orogenic systems: Nature Geoscience, v. 2, p. 251–257.

DeCelles, P.G. and Giles, K.A., 1996, Foreland basin systems: Basin Research, v. 8, p. 105–123.

DeCelles, P.G. and Horton, B.K., 2003, Early to middle Tertiary foreland basin development and the history of Andean crustal shortening in Bolivia: Geological Society of America Bulletin, v. 115, p. 58–77.

De Deckker, P., 2002, Ostracode paleoecology, *in* J.A. Holmes and A.R. Chivas (eds.), The Ostracoda: Applications in the Quaternary Research: Washington, D.C., American Geophysical Union, Geophysical Monograph 131, p. 121–134.

De Deckker, P. and Forester, R.M., 1988, The use of ostracodes to reconstruct continental palaeoenvironmental records, *in* P. De Deckker, J.-P. Colin, and J.-P. Peypouquet (eds.), Ostracoda in the Earth Sciences: Elsevier, New York, p. 175–199.

Forester, R.M., 1988, Nonmarine calcareous microfossils sample preparation and data acquisition procedures: U.S. Geological Survey Technical Procedure HP-78 R1, p. 1–9.

Forester, R.M., 1991, Ostracode assemblages from springs in the western United States: implications for paleohydrology: Memoirs of the Entomological Society of Canada, v. 155, p. 181–201.

Fritz, S.C., Baker, P.A., Lowenstein, T.K., Seltzer, G.O., Rigsby, C.A., Dwyer, G.S., Tapia, P.M., Arnold, K.K., Ku, T.L., and Luo, S., 2004, Hydrologic variation during the last 170,000 years in the southern hemisphere tropics of South America: Quaternary Research, v. 61, p. 95–104.

Fritz, S.C., Baker, P.A., Seltzer, G.O., Ballantyne, A., Tapia, P., Cheng, H., and Edwards, R.L., 2007, Quaternary glaciation and hydrologic variation in the South American tropics as reconstructed from the Lake Titicaca drilling project: Quaternary Research, v. 68, p. 410–420.

Gangui, A.H., 1998, A combined structural interpretation based on seismic data and 3D gravity modeling in the northern Puna/Eastern Cordillera, Argentina: PhD Thesis, Freien Universität, Berlin, 176 p.

Garreaud, R.D., Vuille, M., Compagnucci, R., and Marengo, J., 2009, Present day South American Climate: Palaeogeography, Palaeoclimatology, Palaeoecology, v. 281, p. 180–195.

Goring, S., Williams, J.W., Blois, J.L., Jackson, S.T., Paciorek, C.J., Booth, R.K., Marlon, J.R., Blaauw, M., and Christen, J.A., 2012, Deposition times in the northeastern United States during the Holocene: establishing valid priors for Bayesian age models: Quaternary Science Reviews, v. 48, p. 54–60.

Hammer, Ø., 2013, PAST Paleontological Statistics Version 3.0, Reference Manual: University of Oslo.

Hogg, A.G., Hua, Q., Blackwell, P.G., Buck, C.E., Guilderson, T.P., Heaton, T.J., Niu, M., Palmer, J., Reimer, P.J., Reimer, R., Turney, C.S.M., and Zimmerman, S.R.H., 2013, ShCal13 Southern Hemisphere calibration, 0–50,000 cal yr BP: Radiocarbon, v. 55, doi:10.2458/azu_js_rc.55.16783.

Holmes, J.A., 2008, Sample-size implications of the trace-element variability of ostracod shells: Geochimica et Cosmochima Acta, v. 72, p. 2934–2945.

Holmes, J.A. and Chivas, A.R., 2002, Ostracod shell chemistry—Overview, *in* J.A. Holmes and A.R. Chivas (eds.), The Ostracoda: Applications in Quaternary Research: American Geophysical Union, Geophysical Monograph, v. 131, p. 185–204.

Horne, D.J., Cohen, A., and Martens, K., 2002, Taxonomy, morphology and biology of Quaternary and living Ostracoda, *in* J.A. Holmes and A.R. Chivas (eds.), The Ostracoda: Applications in the Quaternary Research: American Geophysical Union, Geophysical Monograph, v. 131, p. 5–36.

Horton, B.K., 2012, Cenozoic evolution of hinterland basins in the Andes and Tibet, in C.J. Busby and A. Azor (eds.), Tectonics of Sedimentary Basins: Recent Advances, Wiley-Blackwell, Oxford, 664 p.

Hren, M.T. and Sheldon, N.D., 2012, Temporal variations in lake water temperature: paleoenvironmental implications of lake carbonate δ18O and temperature records: Earth and Planetary Science Letters, v. 337, p. 77–84.

Hua, Q., Barbetti, M., and Rakowski, A.Z., 2013, Atmospheric radiocarbon for the period 1950–2010: Radiocarbon, v. 55, p. 2059–2072.

Igarzábal, A.P., 1978, La Laguna de Pozuelos y su Ambiente Salino: Acta Geológica Lilloana, v. 15, p. 80–103.

Kim, S.T., O'Neil, J.R., Hillaire-Marcel, C., and Mucci, A., 2007, Oxygen isotope fractionation between synthetic aragonite and water: influence of temperature and Mg 2+ concentration: Geochimica et Cosmochimica Acta, v. 71, p. 4704–4715.

Krause, W., 1997, Charales (Charophyceae), *in* H. Ettl, G. Gartner, H. Heynig, and D. Mollenhauer (eds.), Sußwasserflora von Mitteleuropa, Gustav Fischer, Jena, v. 18, 202 p.

Laprida, C., Massaferro, J., Ramón Mercau J., and Cusminsky, G.C., 2015, Paleobioindicadores Del Fin Del Mundo: Ostrácodos y Quironómidos Del Extremo Sur De Sudamérica En Ambientes Lacustres Cuaternarios: Latin American Journal of Sedimentology and Basin Analysis, v. 21, p. 2

Legates, D.R. and Willmott, C.J. 1990a, Mean seasonal and spatial variability in gauge-corrected, global precipitation: International Journal of Climatology, v. 10, p. 111–127.

Legates, D.R. and Willmott, C.J., 1990b, Mean seasonal and spatial variability in global surface air temperature: Theoretical Applied Climatology, v. 41, p. 11–21.

Leng, M.J. and Marshall, J.D., 2004, Palaeoclimate interpretation of stable isotope data from lake sediment archives: Quaternary Science Reviews, v. 23, p. 811–831.

Lopez Steinmetz, R.L. and Galli, C.I., 2015, Hydrological change during the Pleistocene–Holocene transition associated with the Last Glacial Maximum-Altithermal in the eastern border of northern Puna: Andean Geology, v. 42, p. 1–19.

McGlue, M.M., Cohen, A.S., Ellis, G.S., and Kowler, A.L., 2013, Late Quaternary stratigraphy, sedimentology and geochemistry of an underfilled lake basin in the Puna plateau (northwest Argentina): Basin Research, v. 25, p. 638–658.

McGlue, M.M., Ellis, G.S., Cohen, A.S., and Swarzenski, P.W., 2012, Playa-lake sedimentation and organic matter accumulation in an Andean piggyback basin: the recent record from the Cuenca de Pozuelos, North-west Argentina: Sedimentology, v. 59, p. 1237–1256.

Mercau, J.R., Laprida, C., Massaferro, J., Rogora, M., Tartari, G., and Maidana, N.I., 2012, Patagonian ostracods as indicators of climate-related hydrological variables: implications for paleoenvironmental reconstructions in Southern South America: Hydrobiologia, v. 694, p. 235–251.

Mourguiart, P. and Corrège, T., 1998, Écologie et paléoécologie des ostracodes actuels et Holocènes de l'Altiplano Bolivien: what about Ostracoda!: Actes du 3e Congrès Européen des Ostracodologistes, 1998, Bulletin Centre Recherche Elf Exploration et Production, Mémoire 20, p. 103–115.

Oertli, H.J., 1971, The aspects of ostracod faunas, a possible new tool in petroleum sedimentology: Bulletin du Centre de Recherche de Pau-SNPA, v. 5, p. 137–151.

Ori, G.G. and Friend, P.F., 1984, Sedimentary basins formed and carried piggyback on active thrust sheets: Geology, v. 12, p. 475–478.

Paduano, G.M., Bush, M.B., Baker, P.A., Fritz, S.C., and Seltzer, G.O., 2003, A vegetation and fire history of Lake Titicaca since the Last Glacial Maximum: Palaeogeography, Palaeoclimatology, Palaeoecology, v. 194, p. 259–279.

Palacios-Fest, M.R., 1994, Nonmarine ostracode shell chemistry from Hohokam irrigation canals in Central Arizona: a paleohydrochemical tool for the interpretation of prehistoric human occupation in the North American Southwest: Geoarchaeology, v. 9, p. 1–29.

Palacios-Fest, M.R., Cohen, A.S., and Anadón, P., 1994, Use of ostracodes as paleoenvironmental tools in the interpretation of ancient lacustrine records: Revista Española de Micropaleontología, v. 9, p. 145–164.

Palacios-Fest, M.R., Cusminsky, G.C., and McGlue, M.M., 2016, Late Quaternary lacustrine ostracods (Ostracoda, Crustacea) and charophytes (Charophyta, Charales) from the Puna Plateau, Argentina: Journal of Micropalaeontology, v. 35, p. 66–78.

Petsch, S.T., Berner, R.A., and Eglinton, T.I., 2000, A field study of the chemical weathering of ancient sedimentary organic matter: Organic Geochemistry, v. 31, p. 475–487.

Placzek, C., Quade, J., and Patchett, P.J., 2006, Geochronology and stratigraphy of late Pleistocene lake cycles on the southern Bolivian Altiplano: implications for causes of tropical climate change: Geological Society of America Bulletin, v. 118, p. 515–532.

Placzek, C.J., Quade, J., and Patchett, P.J., 2013, A 130ka Reconstruction of rainfall on the Bolivian Altiplano: Earth and Planetary Science Letters, v. 363, p. 97–108.

Pokorný, V., 1978, Ostracodes, Chapter 8, *in* B.U. Haq and A. Boersma (eds.), Introduction to Marine Micropaleontology: Elsevier, New York, p. 109–149.

Puri, H.S., 1974, Normal pores and the phylogeny of Ostracoda: Geoscience and Man, v. 6, p. 137–151.

Quade, J., Rech, J.A., Betancourt, J.L., Latorre, C., Quade, B., Rylander, K.A., and Fisher, T., 2008, Paleowetlands and regional climate change in the central Atacama Desert, northern Chile: Quaternary Research, v. 69, p. 343–360.

Ramos, L., Cusminsky, G.C., Schwalb, A., and Alperín, M., 2016, Morphotypes of the lacustrine ostracod *Limnocythere rionegroensis* Cusminsky and Whatley from Patagonia, Argentina, shaped by aquatic environments: Hydrobiologia, doi: 10.1007/s10750-016-2870-z.

Rigsby, C.A., Bradbury, J.P., Baker, P.A., Rollins, S.M., and Warren, M.R., 2005, Late Quaternary palaeolakes, rivers, and wetlands on the Bolivian Altiplano and their palaeoclimatic implications: Journal of Quaternary Science, v. 20, p. 671–691.

Rip, W.J., Ouboter, M.R., and Los, H.J., 2007, Impact of climatic fluctuations on Characeae biomass in a shallow, restored lake in The Netherlands: Hydrobiologia, v. 584, p. 415–424.

Romanov, R.E. and Barinova, S.S., 2012, The charophytes of Israel: historical and contemporary species richness, distribution, and ecology: Biodiversity: Research and Conservation, v. 25, p. 67–74.

Schoenbohm, L.M. and Carrapa, B., 2014, Miocene–Pliocene shortening, extension, and mafic magmatism support small-scale lithospheric foundering in the Central Andes, NW Argentina: Geological Society of America Memoirs, v. 212, p. MWR212-09.

Schwalb, A., 2003, Lacustrine ostracodes as stable isotope recorders of late-glacial and Holocene environmental dynamics and climate: Journal of Paleolimnology, v. 29, p. 265–351.

Schwalb, A., Burns, S.J., Cusminsky, G., Kelts, K., and Margraf, V., 2002, Assemblage diversity and isotopic signals of modern ostracodes and host waters from Patagonia, Argentina: Palaeogeography, Palaeoclimatology, Palaeoecology, v. 187, p. 323–339.

Schwalb A., Burns S.J., and Kelts, K., 1999, Holocene environments from stable isotope stratigraphy of ostracodes and authigenic carbonates in Chilean Altiplano Lakes: Palaeogeography, Palaeoclimatology, Palaeoecology v. 148, p. 153–168.

Seltzer, G.O., Baker, P., Cross, S., Dunbar, R. and Fritz, S., 1998, High-resolution seismic reflection profiles from Lake Titicaca, Peru-Bolivia: evidence for Holocene aridity in the tropical Andes: Geology, v. 26, p. 167–170.

Talbot, M.R., 1990, A review of the palaeohydrological interpretation of carbon and oxygen isotopic ratios in primary lacustrine carbonates: Chemical Geology: Isotope Geoscience Section, v. 80, p. 261–279.

Teller, J.T. and Last, W.M., 1990. Paleohydrological indicators in playas and salt lakes, with examples from Canada, Australia, and Africa: Palaeogeography, Palaeoclimatology, Palaeoecology, v. 76, p. 215–240.

Torres Saldarriaga, A. and Martínez, J.I., 2010, Ecology of non-marine Ostracoda from La Fe Reservoir (El Retiro, Antioquia) and their potential applications in paleoenvironmental studies: Revista Academia Colombiana de Ciencias, v. 34, p. 397–409.

Van den Berg, M.S., Scheffer, M., Van Nes, E., and Coops, H., 1999, Dynamics and stability of *Chara* sp. and *Potamogeton pectinatus* in a shallow lake changing in eutrophication level: Shallow Lakes' 98, Springer, Netherlands, p. 335–342.

Vandervoort, D.S., Jordan, T.E., Zeitler, P.K., and Alonso, R.N., 1995, Chronology of internal drainage development and uplift, southern Puna plateau, Argentine Central Andes: Geology, v. 23, p. 145–148.

von Grafenstein, U., Eicher, U., Erlenkeuser, H., Ruch, P., Schwander, J., and Ammann, B., 2000, Isotope signature of the Younger Dryas and two minor oscillations at Gerzensee (Switzerland): palaeoclimatic and palaeolimnologic interpretation based on bulk and biogenic carbonates: Palaeogeography, Palaeoclimatology, Palaeoecology, v. 159, p. 215–229.

Whatley, R., 1983, Some simple procedures for enhancing the use of Ostracoda in palaeoenvironmental analysis: Norwegian Petroleum Directorate Bulletin, v. 2, p. 129–146.

Whatley, R.C. and Cusminsky, G.C., 1999, Lacustrine ostracoda and late Quaternary palaeoenvironments from the lake Cari-Laufquen region, Rio Negro province, Argentina: Palaeogeography, Palaeoclimatology, Palaeoecology, v. 151, p. 229–239.

Zhou, J. and Lau, K.M. 1998, Does a monsoon climate exist over South America?: Journal of Climatology, v. 11, p. 1020–1040.

Received 20 September 2016; accepted 6 April 2017.